Bioorganic & Medicinal Chemistry 23 (2015) 9–21

Contents lists available at ScienceDirect

Bioorganic & Medicinal Chemistry

journal homepage: www.elsevier.com/locate/bmc

1,2,4-Triazolo[1,5-*a*]quinoxaline derivatives and their simplified analogues as adenosine A_3 receptor antagonists. Synthesis, structure–affinity relationships and molecular modeling studies

Daniela Catarzi [a,*], Flavia Varano [a], Daniela Poli [a], Lucia Squarcialupi [a], Marco Betti [a], Letizia Trincavelli [b], Claudia Martini [b], Diego Dal Ben [c], Ajiroghene Thomas [c], Rosaria Volpini [c], Vittoria Colotta [a]

[a] *Dipartimento di Neuroscienze, Psicologia, Area del Farmaco e Salute del Bambino, Sezione di Farmaceutica e Nutraceutica, Università di Firenze, Polo Scientifico, Via Ugo Schiff 6, 50019 Sesto Fiorentino, FI, Italy*
[b] *Dipartimento di Farmacia, Università di Pisa, Via Bonanno Pisano 6, 56126 Pisa, Italy*
[c] *School of Pharmacy, Medicinal Chemistry Unit, University of Camerino, Via S. Agostino 1, 62032 Camerino (MC), Italy*

ARTICLE INFO

Article history:
Received 22 July 2014
Revised 30 October 2014
Accepted 21 November 2014
Available online 27 November 2014

Keywords:
G protein-coupled receptors
Adenosine receptor antagonists
Triazoloquinoxalines
Tricyclic heteroaromatic systems
Ligand–receptor modeling studies

ABSTRACT

The 1,2,4-triazolo[1,5-*a*]quinoxaline (TQX) scaffold was extensively investigated in our previously reported studies and recently, our attention was focused at position 5 of the tricyclic nucleus where different acyl and carboxylate moieties were introduced (compounds **2**–**15**). This study produced some interesting compounds endowed with good hA_3 receptor affinity and selectivity. In addition, to find new insights about the structural requirements for hA_3 receptor–ligand interaction, the tricyclic TQX ring was destroyed yielding some 1,2,4-triazole derivatives (compounds **16**–**23**). These simplified compounds, though maintaining the crucial structural requirements for adenosine receptor–ligand interaction, have a very low hA_3 adenosine receptor affinity, the only exception being compound **23** (1-[3-(4-methoxyphenyl)-1-phenyl-1*H*-1,2,4-triazol-5-yl]-3-phenylurea) endowed with a K_i value in the micro-molar range and high hA_3 selectivity versus both hA_1 and hA_{2A} AR subtypes. Evaluation of the side products obtained in the herein reported synthetic pathways led to the identification of some new triazolo[1,5-*a*]quinoxalines as hA_3AR antagonists (compounds **24**–**27**). These derivatives, though lacking the classical structural requirements for the anchoring at the hA_3 receptor site, show high hA_3 affinity and in some case selectivity versus hA_1 and hA_{2A} subtypes. Molecular docking of the herein reported tricyclic and simplified derivatives was carried out to depict their hypothetical binding mode to our model of hA_3 receptor.

1. Introduction

Adenosine is a ubiquitous nucleoside that regulates a large number of physiological and patho-physiological processes by triggering specific adenosine receptors (ARs) at the extracellular level. The ARs are four different subtypes of G protein-coupled receptors (GPCRs) classified as A_1, A_{2A}, A_{2B} and A_3 on the basis of their tissue localization, respective coupling to adenylate cyclase (AC) and specific pharmacological criteria.[1]

The adenosine A_3 receptor (A_3AR), the most recently characterized, was originally isolated from rat testis[2] and subsequently cloned from a variety of species.[3] For the A_3AR, significant differences (72%) in sequence similarity and tissue distribution have been observed between species.[4,5] However, this receptor is widely distributed in the human body, both in peripheral organs and in distinct regions of the central nervous system (CNS), though in low levels. The A_3AR is reported to be related to various second messenger systems. Its activation leads to inhibition of AC and stimulation of phospholipase C and D[6,7] through G_i and G_q proteins, respectively. Moreover, additional intracellular pathways have been described to be important for intracellular signal transduction in the adenosine biochemical system.[6,8] The improved understanding of the physiological effects mediated by the A_3AR and of its biology has provided substantial evidence that this AR subtype is an interesting target for different therapeutic interventions. In particular, A_3AR antagonists are being investigated for the treatment of glaucoma, asthma, inflammation[9] and cerebral ischemia.[10,11] A_3AR antagonists have also been reported to have potential efficacy in both glioblastoma multiforme and colon cancer therapy.[12,13]

However, the role of A_3AR antagonists as potential therapeutics in many pathological diseases such as inflammation, cerebral

* Corresponding author. Tel.: +39 055 4573722; fax: +39 055 4573780.
E-mail address: daniela.catarzi@unifi.it (D. Catarzi).

http://dx.doi.org/10.1016/j.bmc.2014.11.033
0968-0896/

ischemia and cancer is still ambiguous and widely debated.[14] Thus, the search for potent and selective human (h) A_3AR antagonists has become an attractive goal for many scientists. In the last few years, much effort has been directed toward design and development of potent and selective AR antagonists belonging to diverse classes of heterocyclic derivatives with different structures.[9]

The 1,2,4-triazolo[1,5-*a*]quinoxaline (TQX) ring system is a recurrent structural core which has been used to obtain tricyclic AR antagonists.[15–18] The first AR antagonists belonging to this series were designed as structural analogues of CGS15943 (9-chloro-2-(2-furanyl)[1,2,4]triazolo[1,5-*c*]quinazolin-5-amine)[19] in the mid-nineties[15] and, since then, many other TQX derivatives of interest have been developed by our research group. In particular, the 8-chloro-2-phenyl-1,2,4-triazolo[1,5-*a*]quinoxalin-4-amine[17] (**1A**, Fig. 1) was modified by introducing suitable substituents either on the 4-amino group or the 2-phenyl ring (**Series A**,[17] Fig. 1). The presence of an acyl moiety on the 4-amino group, as in compound **2A**, led to potent and selective hA_3AR antagonists. The improvement of hA_3 affinity and selectivity was hypothesized to be due to the amide carbonyl at position-4 that can act as a proton acceptor in a hydrogen bonding interaction with a proton donor binding site. A further increase in affinity was observed when a methoxy group which can engage an additional hydrogen bond with the receptor site was introduced in the *para* position of the 2-phenyl substituent.[17]

These promising results indicated that the TQX ring system is a versatile scaffold which can be further modified to develop new AR antagonists. Thus, we studied a series of 2-(hetero)aryl-1,2,4-triazolo[1,5-*a*]quinoxaline derivatives bearing a 4-oxo function replacing the 4-amino group of the previously reported **Series A** (**Series B**,[18] Fig. 1). Some interesting hA_3 AR antagonists were produced starting from the 8-chloro-2-phenyl-4,5-dihydro-1,2,4-triazolo[1,5-*a*]quinoxalin-4-one **1B**, selected as lead compound.[18] Profitable modifications were made either by introducing different aryl and heteroaryl groups at position 2, or by replacing the 8-chloro substituent with a methyl group or a hydrogen atom. In order to further investigate the potentiality of the TQX ring system, we decided to move the 4-carbonyl function of **Series B** into an exonuclear position by introducing different acyl or carboxyalkyl substituents at N-5 (**Series C**, compounds **2**–**15**, Fig. 2). We also introduced the above cited suitable substituents, that is, the 8-chloro or 8-methyl on the fused benzo moiety and the crucial 4-methoxy on the 2-phenyl ring, onto the TQX scaffold.

To find new insights into the structural requirements for hA_3 receptor–ligand interaction, the tricyclic TQX ring was destroyed by eliminating the 4-methylene bridge of **Series C**, generating

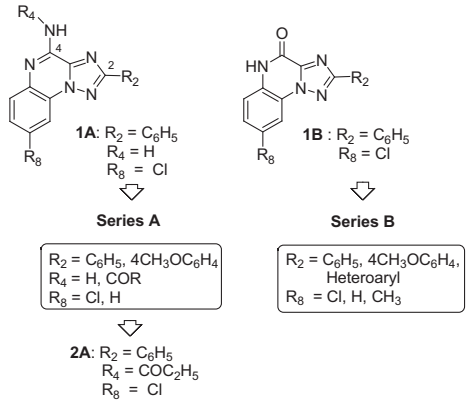

Figure 1. Previously reported 4-amino- and 4-oxo-substituted 2-(hetero)aryl-1,2,4-triazolo[1,5-*a*]quinoxaline (TQX) derivatives as human A_3 adenosine receptor antagonists.

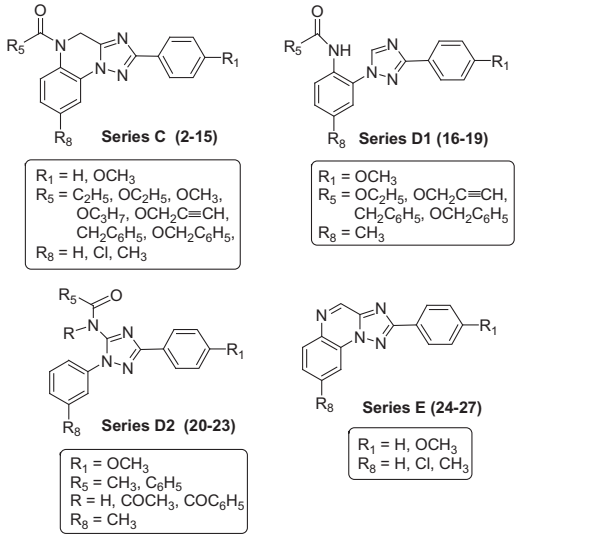

Figure 2. Currently reported 1,2,4-triazolo[1,5-*a*]quinoxaline (TQX) derivatives and their simplified 1,3-diaryl-1,2,4-triazole analogues.

the new 1,3-diaryl-1,2,4-triazole monocyclic core (**Series D1**, compounds **16**–**19**, Fig. 2) which can be considered a simplified structure of **Series C**. Contemporarily, analogues of **Series D1**, called **Series D2** (compounds **20**–**23**), were designed by moving the substituted NH group from the *ortho*-position of the 1-aryl moiety to the 5-position on the 1,2,4-triazole core. Hence, both **Series D1** and **D2** maintain the substituted NH group and the two aryl moieties which could be important requirements for a profitable interaction with the AR binding pockets.[9] It has to be noted that only a few other monocyclic cores have been evaluated as possible candidates for developing AR antagonists.[20–25]

In addition, looking at the side products in the synthetic pathway which leads to the targeted TQX compounds, we have identified the 4,5-dehydro-derivatives (**Series E**, compounds **24**–**27**, Figure 2) as possible candidates for our pharmacological studies. Unlike the other series herein reported, these compounds lack all the classical structural requirements considered important for anchoring at the receptor binding sites, while maintaining only the nude tricyclic TQX scaffold.

2. Chemistry

The synthetic pathways which yielded compounds **2**–**15**, **16**–**19**, **20**–**23** and **24**–**27**[26] are illustrated in Schemes 1–3. Compounds **2**–**15** (**Series C**) were obtained starting from the 2-aryl-4,5-dihydro-1,2,4-triazolo[1,5-*a*]quinoxalin-4-ones **28**–**31**,[18,26] as reported in Scheme 1. Reduction of the 4-oxo function of **28**–**31** with $LiAlH_4$ led to a mixture of the key intermediates **32**–**35**[26] and small amounts of the 4,5-dehydro-derivatives **24**–**27**,[26] which were successively evaluated as AR antagonists. An increased quantity of **25** and **27** was obtained by treating **33** and **35**, respectively, with glacial acetic acid at reflux. Derivatives **32**–**35** were reacted with the suitable acyl chloride or chloroformates in the presence of pyridine to yield the final N-5-substituted compounds **2**–**15**. In order to find an alternative synthetic pathway to achieve the target compounds **32**–**35** with higher yields, we synthesized **35** starting from the 1,3-diaryl-5-chloromethyl-1,2,4-triazole **37** which was obtained by treating the amidrazone **36**[18] with chloroacetyl chloride. The intermediate **37** was transformed into the tricyclic derivative **35** with $SnCl_2$ dihydrate, and only traces of compound **27** were obtained (^{1}H NMR determination). In this way the synthetic procedure for preparing **35** has been shortened and the total yield improved.

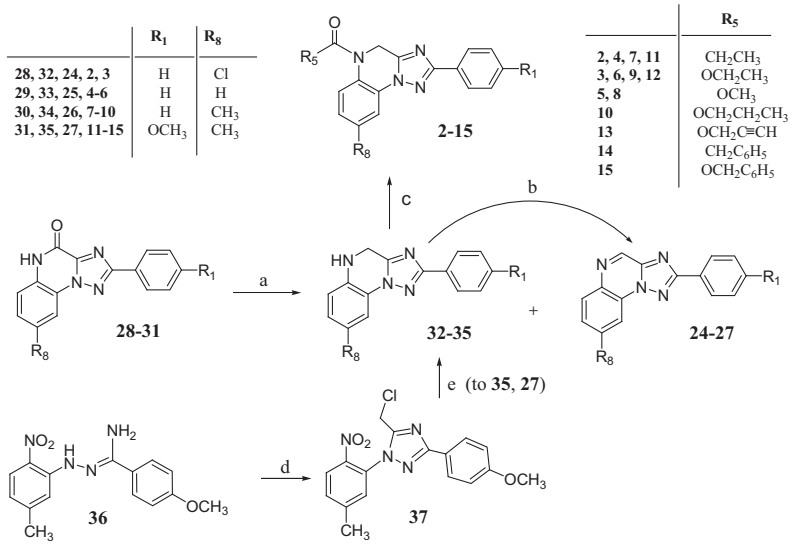

Scheme 1. Reagents and conditions. (a) $LiAlH_4$, anhydrous tetrahydrofuran, nitrogen atmosphere, reflux; (b) glacial acetic acid, reflux; (c) R_5COCl, pyridine, anhydrous dichloromethane, nitrogen atmosphere; (d) $ClCOCH_2Cl$, anhydrous toluene, 80 °C; (e) $SnCl_2$ dihydrate, ethanol, reflux.

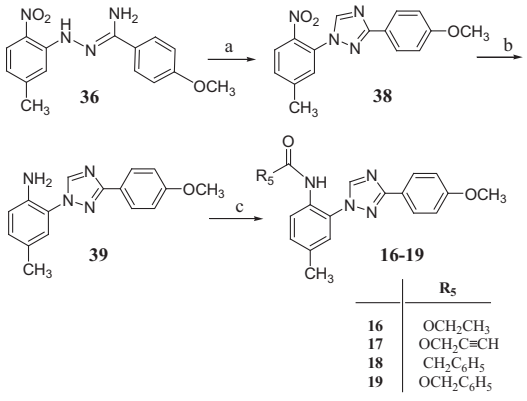

Scheme 2. Reagents and condition: (a) $CH(OEt)_3$, *p*-toluensulfonic acid, 100 °C; (b) 10% Pd/C, H_2, ethyl acetate; (c) R_5COCl, pyridine, anhydrous dichloromethane, 0 °C.

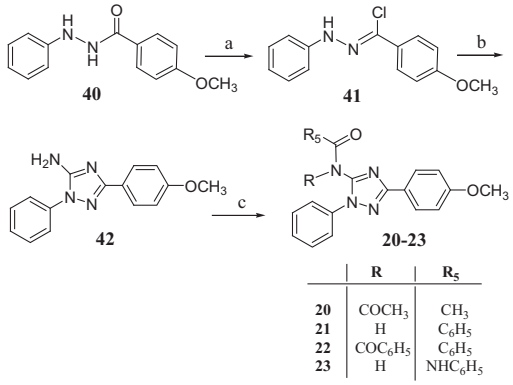

Scheme 3. Reagents and condition. (a) $POCl_3$, PCl_5, reflux; (b) NH_2CN, 100 °C; (c) acetic anhydride, pyridine, reflux; or C_6H_5COCl, pyridine, anhydrous tetrahydrofuran, reflux; or C_6H_5NCO, anhydrous dichloromethane, 5 °C/room temperature.

The simplified 1,2,4-triazole derivatives of **Series D1** (**16**–**19**) were obtained as reported in Scheme 2. Reaction of **36** with triethyl orthoformate in the presence of *para*-toluenesulfonic acid, led to 1,2,4-triazole cyclization (compound **38**). By reduction of the nitro group of **38**, the corresponding amino-derivative **39** was obtained which was reacted with the suitable acyl chloride or chloroformates to provide compounds **16**–**19** with high yields.

The synthesis of compounds **20**–**23** (**Series D2**) was performed as reported in Scheme 3. By reacting the hydrazide **40**[27,28] with a mixture of $POCl_3$ and PCl_5 at reflux, the unstable chloroimine **41**[29] was obtained which was immediately reacted with cyanamide at 100 °C in solvent-free conditions to give the intermediate **42**. Then, the latter was transformed into the corresponding acyl- and carbamoyl-derivatives by reacting with acetic anhydride (compound **20**), benzoyl chloride (**21**, **22**) or phenyl isocyanate (**23**).

3. Pharmacology

The newly synthesized derivatives **2**–**15** (Table 1), **16**–**23** (Table 2), and **24**–**27** (Table 3) were tested for their ability to displace [^{125}I]N^6-(4-amino-3-iodobenzyl)-5′-(*N*-methylcarbamoyl)adenosine ([^{125}I]AB-MECA) from a cloned hA_3 receptor stably expressed in CHO cells. Subsequently, all compounds except **3** and **25**, were evaluated for their ability to displace [^{3}H]8-cyclopentyl-1,3-dipropylxantine ([^{3}H]DPCPX) from cloned hA_1 ARs, and [^{3}H]5′-(*N*-ethylcarboxamido)adenosine ([^{3}H]NECA) from cloned hA_{2A} ARs, to establish their A_3 versus A_1 and versus A_{2A} selectivity. In Table 1, the binding results of the reference compound **1B**[18] (Fig. 1) at hA_3 AR is reported.

To determine hA_3 versus hA_{2B} selectivity, some selected compounds (**2**, **7**–**9**, **11**, **13**–**14**, **27**) were tested at the hA_{2B} subtype by measuring their effects on cyclic adenosine monophosphate (cAMP) accumulation in CHO cells stably transfected with the hA_{2B} AR (Table 4).

4. Results and discussion

4.1. Structure–affinity relationships

The binding results reported in Tables 1–3 indicate that we have produced some new potent and selective hA_3 AR antagonists belonging to the 1,2,4-triazolo[1,5-*a*]quinoxaline series (**Series C** and **E**, Table 1 and 3, respectively). Some of the novel derivatives show high hA_3 AR affinity (K_i <100 nM) and selectivity versus the hA_{2A} receptor (compounds **2**, **7**–**9** and **11**–**14**) and, in some cases, also good selectivity versus the hA_1 subtype. The choice to test

Table 1
Binding affinity (K_i) at hA_3, hA_1 and hA_{2A} ARs of the 5-substituted 2-aryl-4,5-dihydro-1,2,4-triazolo[1,5-*a*]quinoxaline derivatives (**Series C**)

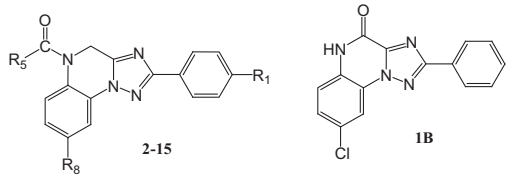

	R_1	R_5	R_8	K_i[a] (nM) or I%		
				hA_3[b]	hA_1[c]	hA_{2A}[d]
2	H	C_2H_5	Cl	72 ± 6.8	39%	24%
3	H	OC_2H_5	Cl	166 ± 15	n.d.	n.d.
4	H	C_2H_5	H	55%	1360 ± 50	52%
5	H	OCH_3	H	245 ± 24	34%	50%
6	H	OC_2H_5	H	22%	4600 ± 118	33%
7	H	C_2H_5	CH_3	6.5 ± 0.5	134.3 ± 7	33%
8	H	OCH_3	CH_3	31.9 ± 3	1481 ± 145	32%
9	H	OC_2H_5	CH_3	12.5 ± 1.1	556 ± 55	9%
10	H	OC_3H_7	CH_3	171 ± 16	565 ± 72	56%
11	OCH_3	C_2H_5	CH_3	25.1 ± 2	1543 ± 61	6%
12	OCH_3	OC_2H_5	CH_3	39.4 ± 3	86 ± 8	2%
13	OCH_3	$OCH_2C{\equiv}CH$	CH_3	23.3 ± 1.8	49%	13%
14	OCH_3	$CH_2C_6H_5$	CH_3	54.8 ± 5	39%	0%
15	OCH_3	$OCH_2C_6H_5$	CH_3	231.4 ± 18	45%	4%
1B[e]	—	—	—	163 ± 13	n.d.	n.d.

[a] K_i values are means ± SEM of four separate assays, each performed in triplicate.
[b] Displacement of specific [^{125}I]AB-MECA binding at hA_3 receptors expressed in CHO cells or percentage of inhibition (I%) of specific binding at 1 μM.
[c] Displacement of specific [^{3}H]DPCPX binding at hA_1 receptors expressed in CHO cells or percentage of inhibition (I%) of specific binding at 10 μM concentration.
[d] Percentage of inhibition (I%) of specific [^{3}H]NECA binding at hA_{2A} receptors expressed in CHO cells, at 10 μM concentration.
[e] Ref. 18.

Table 2
Binding affinity (K_i) at hA_3, hA_1 and hA_{2A} ARs of the simplified 1,3-diaryl-1,2,4-triazole analogues (**Series D1** and **D2**)

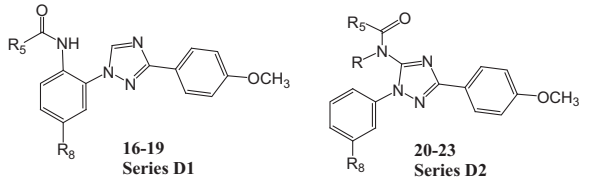

	R	R_5	R_8	K_i[a] (nM) or I%		
				hA_3[b]	hA_1[c]	hA_{2A}[d]
16	—	OC_2H_5	CH_3	34%	6%	13%
17	—	$OCH_2C{\equiv}CH$	CH_3	35%	n.d.	16%
18	—	$CH_2C_6H_5$	CH_3	45%	44%	1%
19	—	$OCH_2C_6H_5$	CH_3	47%	2%	7%
20	$COCH_3$	CH_3	H	19%	26%	4%
21	H	C_6H_5	H	50%	25%	43%
22	COC_6H_5	C_6H_5	H	44%	55%	13%
23	H	NHC_6H_5	H	545 ± 48	1%	7%

[a] K_i values are means ± SEM of four separate assays, each performed in triplicate.
[b] Displacement of specific [^{125}I]AB-MECA binding at hA_3 receptors expressed in CHO cells or percentage of inhibition (I%) of specific binding at 1 μM.
[c] Percentage of inhibition (I%) of specific [^{3}H]DPCPX binding at hA_1 receptors expressed in CHO cells, at 10 μM concentration.
[d] Percentage of inhibition (I%) of specific [^{3}H]NECA binding at hA_{2A} receptors expressed in CHO cells, at 10 μM concentration.

Table 3
Binding affinity (K_i) at hA_3, hA_1 and hA_{2A} ARs of the 1,2,4-triazolo[1,5-*a*]quinoxaline derivatives (**Series E**)

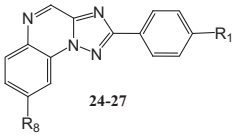

	R_1	R_8	K_i[a] (nM) or I%		
			hA_3[b]	hA_1[c]	hA_{2A}[d]
24	H	Cl	15.2 ± 1.6	127.4 ± 13	19%
25	H	H	91.5 ± 8.9	n.d.	n.d.
26	H	CH_3	23.9 ± 2.19	1322 ± 135	2401 ± 246
27	OCH_3	CH_3	26.6 ± 1	2016 ± 100	30%

[a] K_i values are means ± SEM of four separate assays each performed in triplicate.
[b] Displacement of specific [^{125}I]AB-MECA binding at hA_3 receptors expressed in CHO cells.
[c] Displacement of specific [^{3}H]DPCPX binding at hA_1 receptors expressed in CHO cells.
[d] Displacement of specific [^{3}H]NECA binding at hA_{2A} receptors expressed in CHO cells or percentage of inhibition (I%) of specific binding at 10 μM concentration.

the side products **24**–**27** (**Series E**, Table 3) which turned out to be potent hA_3AR antagonists and, in the case of **26** and **27** also selective versus both the hA_1 and hA_{2A} subtypes in the binding assays was fortunate. In contrast, the simplified 1,2,4-triazole derivatives (**Series D1** and **D2**, Table 2) were inactive or had very low activity at all the AR subtypes, the only exception being compound **23** endowed with a K_i value at the hA_3AR in the micromolar range and high selectivity versus both hA_1 and hA_{2A} subtypes.

Focusing on the results reported in Table 1, we can observe that elimination of the 8-chloro substituent is detrimental for hA_3 receptor–ligand interaction (compare **2** and **3** to **4** and **6**, respectively), while its replacement with a methyl group leads to a strong increase in hA_3 affinity (compare compounds **7** and **9** to **2** and **3**, respectively) and maintains good hA_3 selectivity versus both hA_1 and hA_{2A} receptors. High hA_3 AR binding activity is also observed for compounds **11**–**14** which hold the methyl group at position 8 but, unlike derivatives **7**–**10**, are decorated with a *para*-methoxy group on the 2-phenyl ring. These modifications maintain very high selectivity versus both the hA_{2A} and the hA_1 ARs, the only exception being compound **12** which shows, compared to the parent **9**, a dramatic increase in hA_1 AR affinity and a total loss of hA_3 versus hA_1 selectivity. Nevertheless, the introduction of the *para*-methoxy group does not exert the positive effect on hA_3 affinity observed in the previously reported **Series A** and **B**[17,18] (Fig. 1). In fact, it has to be noted that compounds **11** and **12** possess a 3-fold reduced hA_3 affinity compared to **7** and **9**.

A comparison of the binding data of the previously reported **1B** (Fig. 1) with those of the 5-substituted herein reported (compounds **2**–**15**) highlights that the hA_3 binding affinities of **2**–**15** are similar or higher than that of **1B**, with the only exceptions being the 8-unsubstituted derivatives **4**, **5** and **6** and compound **15** which are less active. These data suggest that replacement of the 4-carbonyl function of **Series B** with exonuclear acyl or carboxyalkyl groups is well tolerated by the hA_3 receptor.

The effect on hA_3 AR affinity and selectivity exerted by the substituents inserted at position 5 of the TQX scaffold is very difficult to explain. By restricting our attention to the 8-methyl substituted compounds **7**–**15**, we can observe that the binding affinity is maintained in the nanomolar range apart from the nature of the substituent at position-5. Hence, the steric hindrance at this position does not seem to be critical for receptor–ligand interaction. It is worth noting that the 5-*N*-propionyl substituted derivative **7** is the most active compound at the hA_3 AR with a K_i value of 6.5 nM (Table 1). Furthermore, compound **13**, bearing the propargyl carboxylate group at the same position, is about 3.5-fold less active than **7**, but much more selective versus the hA_1 subtype.

The opening of the tricyclic TQX scaffold of **Series C** to produce the 1,3-diaryl-1,2,4-triazole system (**Series D1**, Table 2) is

Table 4
Effect of some selected compounds on cAMP production in CHO cells expressing hA_{2B} AR[a]

	% of cAMP production[b]
2	63.7 ± 4.7
7	68.6 ± 4.6
8	74.9 ± 6.3
9	103.8 ± 5.1
11	102.4 ± 6.7
13	108.9 ± 10.2
14	89.5 ± 8.3
27	42.6 ± 1.9

[a] The effect of each compound at 10 μM concentration was evaluated. Each compound was tested in the presence of an EC_{50} concentration of agonist NECA (100 nM, determined on the same day as each assay).
[b] Data are expressed as percentage of cAMP production versus agonist set to 100%. All data represent the mean ± SEM of two different experiments each performed in duplicate.

detrimental for hA_3 AR affinity, although the resulting compounds (**16**–**19**) maintain some ability to bind the hA_3 subtype (35 < I% < 50). Similar results were obtained when the substituted amino group was moved from the 1-aryl-moiety of **Series D1** to the 5-position of the 1,2,4-triazole core (compounds **20**–**23**, **Series D2**, Table 2). However, in contrast with the low hA_3 AR affinity (19 < I% < 50) of the 5-amido-derivatives **20**–**22**, there is the micromolar hA_3 K_i value and high selectivity versus both hA_1 and hA_{2A} subtypes of compound **23**. Thus, this compound could represent a suitable lead for the development of hA_3 AR antagonists endowed with a small heterocyclic core.

In contrast to compounds **16**–**23** (**Series D1** and **D2**), derivatives **24**–**27** (**Series E**, Table 3) hold the tricyclic ring system constant but lack both the claimed NH function and the carbonyl group which are considered important requirements for AR-ligand interaction.[9] Although these derivatives have only the endonuclear nitrogen atoms able to give hydrogen bonding interactions, they show high hA_3 affinity and in some cases selectivity versus hA_1 and hA_{2A} subtypes.

This series also confirms the profitable effect of the presence of a small substituent (chloro or methyl) on the fused benzo moiety for hA_3 receptor–ligand interaction. In fact, the 8-chloro- and 8-methyl-substituted compounds **24** and **26**, respectively, are equipotent at the hA_3AR with a K_i value in the nanomolar range and are 4-6-fold more active than the unsubstituted derivative **25**. These data suggest that these small lipophilic groups could positively interact with a hydrophobic receptor pocket. The presence of a *para*-methoxy substituent on the 2-phenyl ring (compound **27**) is not cooperative as in **Series A** and **B**, leaving unchanged the ability to bind the hA_3AR compared to compound **26**.

To evaluate the hA_3 versus hA_{2B} selectivity, the affinities of some selected derivatives (**2**, **7**–**9**, **11**, **13**–**14**, **27**) at the hA_{2B} AR were evaluated by cAMP functional assay using A_{2B} transfected cells. In general, all the compounds tested alone are not effective in stimulating cAMP accumulation (data not shown). In addition, they showed low or null ability to inhibit cAMP accumulation evoked by the agonist NECA (Table 4). Thus, this study demonstrates that the tested derivatives **2**, **7**–**9**, **11**, **13**–**14**, **27** have not agonist/antagonist activity toward A_{2B} AR subtype.

All together these data confirm that this work produced some compounds endowed with good hA_3 affinity and also selectivity versus all the other ARs.

4.2. Molecular modeling studies

To define the structural features at the basis of the different binding affinities of the new derivatives, a molecular docking analysis was performed on homology models of hA_3AR developed by using four X-ray structures of the antagonist-bound hA_{2A} AR as templates (pdb code: 3EML; 2.6-Å resolution;[30] pdb code: 3PWH; 3.3-Å resolution;[31] pdb code: 3REY; 3.3-Å resolution;[31] pdb code: 3UZA; 3.3-Å resolution[32]). The A_{2A}AR crystal structure provides improved accuracy of AR homology models, due to high residue conservation in the primary sequences of the AR subtypes, which share a sequence identity of ~57% within the transmembrane (TM) domains.[33] The residues located within the seven TM domains in the upper part of ARs, corresponding to the ligand binding site, are conserved with an average identity of 71%.[34] Furthermore, the above cited A_{2A}AR crystal structures have been solved in complex with high affinity antagonists (ZM241385, XAC, and the 6-(2,6-dimethylpyridin-4-yl)-5-phenyl-1,2,4-triazin-3-amine, see cited articles for details), hence presenting a cavity suitable as a binding site for docking analysis. Each obtained hA_3AR homology model was checked by using the Protein Geometry Monitor application within MOE[35] and then employed for a preliminary docking analysis performed by manually docking the high affinity antagonist MRS 1220 (*N*-[9-chloro-2-(2-furyl)[1,2,4]-triazolo[1,5-*c*]quinazolin-5-yl]benzene acetamide, K_i hA_3AR = 0.65 nM[36]) structure within the respective binding site. The obtained hA_3AR–MRS 1220 complexes were then subjected to energy minimization and to Monte Carlo analysis to explore the favorable binding conformations. During this analysis, the ligand was left free to be continuously re-oriented and re-positioned within the binding site and the conformation of both ligand and nearby residues could be explored and reciprocally relaxed. The remaining receptor atoms were kept fixed. This stage was crucial to provide A_3AR binding sites with conformations able to accommodate the analyzed antagonists. For each A_3AR model, the best receptor–MRS 1220 complex was saved and energetically minimized.

Once the MRS 1220 compound was removed, each hA_3AR model was then used as target for the docking analysis of the synthesized derivatives. All ligand structures were optimized using RHF/AM1 semi-empirical calculations (with the aid of the software package MOPAC[37] implemented in MOE) and then docked into the binding site of the hA_3AR models by using the MOE Dock tool. Top-score docking poses of each compound were subjected to energy minimization and then rescored using three available methods implemented in MOE: the *London dG* scoring function, the *Affinity dG* scoring tool, and the *dock-pK_i* predictor. For each compound, the four top-score docking poses, according to at least two out of three scoring functions, were selected for final ligand-target interaction analysis.

The four developed hA_3AR models present highly similar binding sites by considering both pocket volumes and receptor residues orientation. In particular, the binding pockets present only subtle rearrangements of some flexible residues, while the EL domains in peripheral regions of binding site contain higher conformational variability. For example, the side chain of hA_{2A} AR Asn250 (a critical residue for ligand interaction due to its position in the core of the binding pocket) is observed as having different conformations by comparing the hA_{2A} AR crystal structures used as templates and analogue variability is obtained within the developed hA_3AR models for the same amino acid (Asn250). Furthermore, the different interaction and distance between EL2 and EL3 domains (even due to a different orientation of Glu169) are observed in the hA_{2A} AR X-ray structures and also in the developed hA_3AR models. Consequently, it is not surprising that the docking analysis of the synthesized compounds at the four receptor models led to analogue results.

Considering the general binding mode of TQX derivatives belonging to **Series C** (compounds **2**–**15**) in the hA_3AR, two main sets of docking conformations were observed in all four hA_3AR models. Figures 3 and 4 show the binding modes at the hA_3 AR model of compounds **7** as representative of **Series C** compounds.

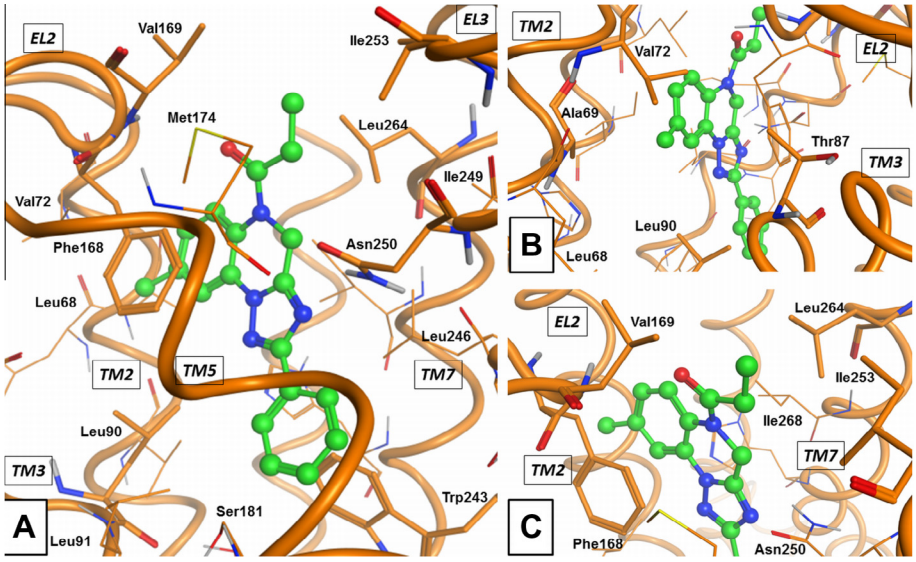

Figure 3. Panel A. Family 1 docking conformations. The binding mode of compound **7** at 3EML-based hA_3AR model is shown as example. Panels B and C. Detailed view of ligand-target interaction considering the 8- and the 5-substituent, respectively.

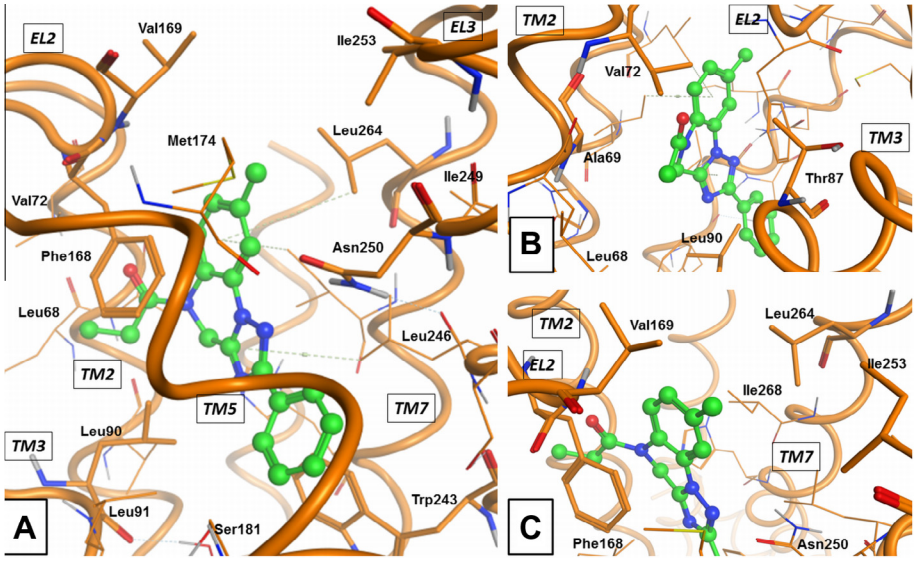

Figure 4. Panel A. Family 2 docking conformations. The binding mode of compound **7** at 3EML-based hA_3AR model is shown as example. Panels B and C. Detailed view of ligand-target interaction considering the 5- and the 8-substituent, respectively.

The first set of conformations (from now on called 'family 1' conformations, Fig. 3, Panel A) presents the TQX moiety located in the center of the binding site with the quinoxaline ring being positioned between Phe168 (EL2) and Ile268 (TM7) side chains. The 2-substituent points towards the central transmembrane core and is located in a mainly hydrophobic subpocket in proximity of Leu90 and Leu91 (TM3), Met177 (TM5), Trp243 and Leu246 (TM6), while the fused phenyl ring is internally oriented and located in a region given by Ala69 and Val72 (TM2), Leu90 (TM3), Phe168 (EL2), and Ile268 (TM7) residues.

Superimposition of the family 1 docking conformations of each compound in the four hA_3AR models shows that the binding modes and the interactions are almost identical at the four binding sites. These conformations are only marginally influenced by the slight rearrangement of external binding site residues as shown by the comparison of the four models. The interaction with the binding site is mainly hydrophobic, the unique exception being given by a possible H-bond between a nitrogen atom of the triazole core and the polar hydrogen of the amide function of Asn250 (TM6) residue. The presence of small substituents on the 2-phenyl ring modulates the interaction with TM5-6 residues, while small groups inserted at the 8-position provide an additional hydrophobic interaction with TM2-3 amino acids. A detailed view of the interaction of compound **7** (taken as template of **Series C**) with the hA_3 AR model is depicted in Figure 3, Panels B and C. The presence of substituents at the 5-position (hence linked to the nitrogen atom of the quinoxaline ring) seems important but not critical for compound activity. The presence of small hydrophobic groups at this position improves the affinity for the receptor; this is not surprising and has already been shown even in the case of hA_3AR agonists.[38–41] Binding data indicate that, on the whole, the propionyl group (COEt) (compounds **2**, **7**, **11**) or the ethyl (COOEt, compounds **3**, **9**, **12**) and methyl (COOMe, **5** and **8**) carboxylate chain at the 5-position have a good effect on compound affinity. This is

particularly true for derivatives bearing an 8-substituent, and can be considered true on the basis of the docking scores of the respective compounds. In the family 1 docking conformations, the phenyl group on the 5-substituent of compounds **14** and **15** is inserted between the hydrophobic side chains of Val169 (EL2) and Ile264 (TM7).

The second set of conformations ('family 2', Fig. 4, Panel A) is a mirror version of family 1, with analogue location of both the TQX scaffold and the 2-substituent, but with the fused phenyl ring pointing externally and located between Met174, Phe168, and Val169 (EL2), Ile249 and Ile253 (TM6), and Leu264 (TM7).

Just as for the family 1 conformations, the interaction with the binding site is mainly hydrophobic, the unique exception being a possible H-bond between a nitrogen atom of the triazole core and the polar hydrogen of the amide function of Asn250 (TM6) residue. The position and role of eventual small substituents on the 2-phenyl ring is analogous to family 1 conformations. Interestingly, the small groups, inserted at the 8-position and externally oriented, are located in analogous positions of the (small) 5-substituents in family 1 conformations. Conversely, the 5-substituents are positioned in an analogous position of 8-substituents in the case of family 1 conformations. Superimposition of the family 2 docking conformations of each compound on the four A_3AR models shows that there are also some differences in compound orientation. The resulting family 2 conformations for compounds **14** and **15** present the tricyclic scaffold more externally oriented with the loss of H-bond interaction with Asn250. Moreover, the phenyl group on the 5-substituent of **14** and **15** could make the family 2 conformations for these two compounds difficult as there is not enough space to accommodate the 5-substituents in the subcavity between TM2 and TM3. This difficulty can be particularly evidenced for compound **15** that is endowed with reduced hA_3 binding activity compared to most of the other N-5 substituted TQX derivatives. Thus, the lower affinity of this compound could be ascribed to its lower ability to assume both binding modes.

All together, the modeling results suggest that the compounds interact with the binding site through generally hydrophobic contact without the presence of strong H-bond or electrostatic interactions. On the other hand, the ability to present two reasonable ways of binding could be the key factor that leads to a higher affinity for the receptor. This result is particularly true for the compounds bearing the 8-substituent and small groups at N-5, for which the two docking conformations are almost equivalent from both the energy and score points of view. Compounds **24**–**27** seem able to assume both conformations as well, and the presence of the 8-substituent provides higher affinity (compare **24** and **26** to **25**).

A docking analysis was performed also to simulate the possible binding modes of the simplified triazole derivatives **16**–**23** at the hA_3AR binding site. The same docking and post-docking protocols were employed. Among these derivatives, only compound **23** showed nanomolar affinity at the hA_3AR. The highest docking score conformation of this compound shows some similarities with family 1 conformations of tricyclic compounds described above. In particular, the triazole ring and the 3-aryl substituent of **23** are located in an analogous position of the triazole ring and the 2-substituent of the tricyclic derivatives **2**–**15**, respectively. The 1-aryl ring mimics the role of the fused phenyl ring of the above described compounds, while the phenyl-urea function of **23** is externally oriented, with the phenyl ring inserted between Val169 (EL2) and Leu264 (TM7). An H-bond interaction occurs between the 4-nitrogen of triazole and a polar hydrogen atom of Asn250 (TM6) and we cannot exclude a possible second interaction involving a polar hydrogen atom of the compound urea function and the Asn250 carbonyl group. Among the monocyclic derivatives described in this work, compound **23** seems the only derivative

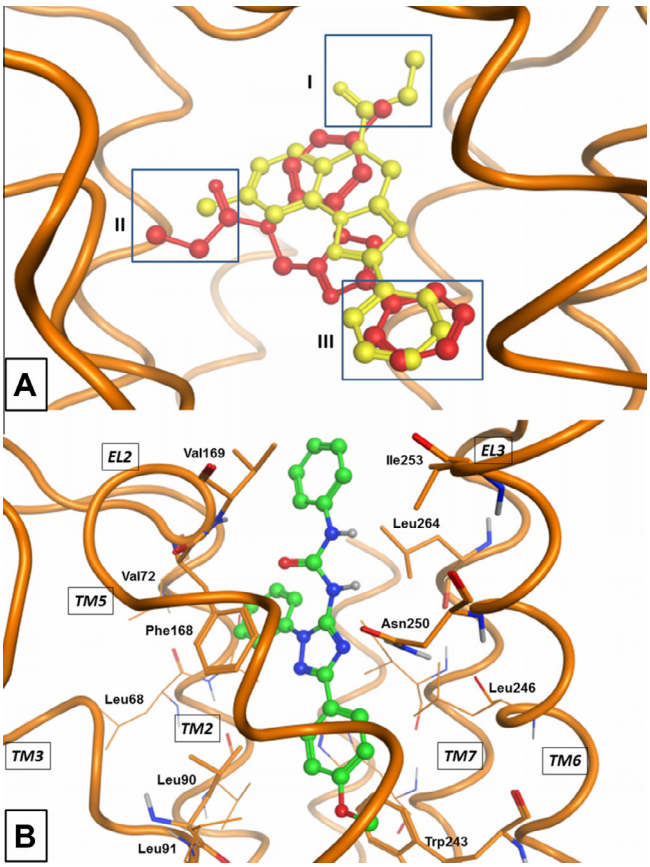

Figure 5. Panel A. Superimposition of family 1 (light) and 2 (dark) docking conformations. The binding mode of compound **7** at 3EML-based hA_3AR model is shown as example. The superimpositions of 5- and 8-substituents (I and II) and 2-substituents (III) are highlighted. Panel B. Docking conformations of simplified triazoles (compound **23**) at 3EML-based hA_3AR model.

able to fit the three subpockets of the hA_3AR binding site indicated as I-III in Figure 5, Panel A, while the other simplified derivatives **16**–**19**, lacking the side chain at the 5-position, do not seem able to properly interact with the binding site.

5. Conclusion

The present study has led to the identification of some 1,2,4-triazolo[1,5-*a*]quinoxalines as new hA_3AR antagonists. In particular, the 5-substituted-4,5-dihydro derivatives **2**–**15** show, on the whole, good hA_3 receptor affinity and in some cases selectivity versus all the other AR subtypes. Surprisingly, similar results are obtained with some TQX compounds (**24**–**27**), obtained as side products, which lack all the classical structural requirements for anchoring at the hA_3 receptor site, and maintain only the nude tricyclic scaffold. In contrast, the 1,2,4-triazole derivatives **16**–**23**, designed as simplified structures from TQX compounds and preserving both the crucial NH and carbonyl groups and the two aryl moieties, turn out to be inactive or have very little activity at all the AR subtypes. The only exception is compound **23** which is endowed with micromolar hA_3AR affinity and high selectivity versus both hA_1 and hA_{2A} subtypes. As a new finding, this triazole derivative emerges as lead candidate for the development of new monocyclic AR antagonists. On the whole, our results lead to new interesting insights about the structural requirements for hA_3 receptor–ligand interaction. Molecular docking of tricyclic and simplified derivatives identify their hypothetical binding mode to our hA_3 receptor model.

6. Experimental section

6.1. Chemistry

Silica gel plates (Merck F254) and silica gel 60 (Merck; 70–230 mesh) were used for analytical and column chromatography, respectively. All melting points were determined on a Gallenkamp melting point apparatus. Microanalyses were performed with a Flash E1112 Thermofinnigan elemental analyzer for C, H, N, and the results were within ±0.4% of the theoretical values except where stated otherwise. All final compounds revealed a purity not less than 95%. The IR spectra were recorded with a Perkin–Elmer Spectrum RX I spectrometer in Nujol mulls and are expressed in cm^{-1}. The ^1H NMR spectra were obtained with a Bruker Avance 400 MHz instrument. The chemical shifts are reported in δ (ppm) and are relative to the central peak of the solvent. The coupling constant (J) are expressed in Hz. All the exchangeable protons were confirmed by addition of D_2O. The following abbreviations are used: s = singlet, d = doublet, dd = double doublet, t = triplet, m = multiplet, br = broad, ar = aromatic protons.

6.1.1. General procedure for the synthesis of 8-substituted 2-aryl-4,5-dihydro-1,2,4-triazolo[1,5-*a*]quinoxalines (32–35)[26] and the corresponding 4,5-dehydro-derivatives (24–27)[26]

To a solution of the previously reported 2-aryl-4,5-dihydro-1,2,4-triazolo[1,5-*a*]quinoxalin-4-ones **28**–**31**[18,26] (2.7 mmol) in anhydrous tetrahydrofuran (200 mL), heated at reflux under nitrogen atmosphere, an excess (21.5 mmol) of $LiAlH_4$ was added portion by portion. At the end of the addition, the reaction mixture was maintained at reflux for 30 min. Then ice (200 g) was carefully added and the mixture was kept under stirring until gas evolution ended. The aqueous phase was extracted with ethyl acetate (100 mL × 2), and the separated organic layers were washed with water (60 mL × 2), anhydrified (Na_2SO_4) and evaporated under reduced pressure. The crude mixture, composed by the 4,5-dihydro-derivatives **32**–**35** and the corresponding dehydro-compounds **24**–**27**, was separated by silica gel column chromatography, eluting system chloroform/methanol 9.5:0.5 (**24** and **32**), chloroform/methanol 9:1 (**25** and **33**), chloroform/acetone 8:2 (**26** and **34**), dichloromethane/cyclohexane/ethyl acetate 9:0.5:0.5 (**27** and **35**).

6.1.1.1. 8-Chloro-2-phenyl-4,5-dihydro-1,2,4-triazolo[1,5-*a*]quinoxaline (32). Yield: 24%; mp 176–178 °C dec (ethanol). ^1H NMR (DMSO-d_6) δ: 4.78 (s, 2H, CH_2), 6.74 (s, 1H, NH), 6.85 (d, 1H, ar J = 8.79), 7.12 (d, 1H, ar, J = 8.06), 7.49–7.58 (m, 4H, ar), 8.08–8.10 (m, 2H, ar). IR: 3295. Anal. Calcd for ($C_{15}H_{11}ClN_4$): C, 63.72; H, 3.92; N 19.82; Found: C, 62.99; H, 3.41; N, 19.98.

6.1.1.2. 2-Phenyl-4,5-dihydro-1,2,4-triazolo[1,5-*a*]quinoxaline (33). Yield: 30%; mp 126–128 °C (ethyl acetate) (lit. mp 126–128 °C).[26]

6.1.1.3. 8-Methyl-2-phenyl-4,5-dihydro-1,2,4-triazolo[1,5-*a*]quinoxaline (34). Yield: 37%; mp 177–179 °C (ethanol). ^1H NMR (DMSO-d_6) δ: 2.26 (s, 3H, CH_3), 4.68 (s, 2H, CH_2), 6.36 (s, 1H, NH), 6.75 (d, 1H, ar, J = 8,06), 6.88 (d, 1H, ar, J = 8.06), 7.44–7.54 (m, 4H, ar), 8.05–8.10 (m, 2H, ar). IR 3300. Anal. Calcd for ($C_{16}H_{14}N_4$): C, 73.26; H, 5.38; N 21.36; Found: C, 73.58; H, 4.71; N, 20.87.

6.1.1.4. 2-(4-Methoxyphenyl)-8-methyl-4,5-dihydro-1,2,4-triazolo[1,5-*a*]quinoxaline (35). Yield: 35% (impure); ^1H NMR (DMSO-d_6) δ: 2.27 (s, 3H, CH_3), 3.83 (s, 3H, OCH_3), 4.67 (s, 2H, CH_2), 6.32 (s, 1H, NH), 6.75 (d, 1H, ar, J = 8.19), 6.89 (d, 1H, ar, J = 8.17 Hz), 7.06 (d, 2H, ar, J = 8.53), 7.43 (s, 1H, ar), 8.01 (d, 2H, ar, J = 8.57). Anal. Calcd for ($C_{17}H_{16}N_4O$): C, 69.85; H, 5.52; N 19.17; Found: C, 70.12; H, 5.75; N, 19.32.

6.1.1.5. 8-Chloro-2-phenyl-1,2,4-triazolo[1,5-*a*]quinoxaline (24). Yield: 24%; mp 217–219 °C (ethyl acetate). ^1H NMR (DMSO-d_6) δ: 7.58–7.61 (m, 3H, ar), 7.86 (dd, 1H, ar, J = 8.79, 2.2), 8.25–8.35 (m, 3H, ar), 8.52 (d, 1H, ar, J = 2.2), 9.51 (s, 1H, ar). IR: 1090, 820. Anal. Calcd for ($C_{15}H_9ClN_4$): C, 64.18; H, 3.23; N 19.96; Found: C, 64.86; H, 3.74; N, 20.13.

6.1.1.6. 2-Phenyl-1,2,4-triazolo[1,5-*a*]quinoxaline (25). Yield: 5%; mp 174–176 °C (ethanol) (lit. mp 181–183 °C).[26]

6.1.1.7. 8-Methyl-2-phenyl-1,2,4-triazolo[1,5-*a*]quinoxaline (26). Yield: 10%; mp 162–164 °C (ethanol). ^1H NMR (DMSO-d_6) δ: 2.64 (s, 3H, CH_3), 7.58–7.66 (m, 4H, ar), 8.13 (d, 1H, ar, J = 8.06), 8.29–8.32 (m, 3H, ar), 9.40 (s, 1H, ar). Anal. Calcd for ($C_{16}H_{12}N_4$): C, 73.83; H, 4.65; N 21.52; Found: C, 74.23; H, 4.05; N, 20.97.

6.1.1.8. 2-(4-Methoxyphenyl)-8-methyl-1,2,4-triazolo[1,5-*a*]quinoxaline (27). Yield: 30%; mp 180–182 °C (cyclohexane). ^1H NMR (DMSO-d_6) δ: 2.65 (s, 3H, CH_3), 3.87 (s, 3H, OCH_3), 7.16 (d, 2H, ar, J = 8.59), 7.64 (d, 1H, ar, J = 8.16), 8.13 (d, 1H, ar, J = 8.24), 8.25 (d, 2H, ar, J = 8.56), 8.32 (s, 1H, ar), 9.38 (s, 1H, CH). Anal. Calcd for ($C_{17}H_{14}N_4O$): C, 70.33; H, 4.86; N 19.30; Found: C, 69.76; H, 5.01; N, 19.12.

6.1.2. Synthesis of 2-Phenyl-1,2,4-triazolo[1,5-*a*]quinoxalines (25, 27)

A mixture of compounds **25**, **33** or **27**, **35** (0.2 g) in glacial acetic acid (5 mL) was heated at reflux for 5 h. Evaporation of the solvent at reduced pressure to small volume produced separation of a solid which was collected and washed with diethyl ether.

2-Phenyl-1,2,4-triazolo[1,5-*a*]quinoxaline (**25**).[26] Yield: 26%.

2-(4-Methoxyphenyl)-8-methyl-1,2,4-triazolo[1,5-*a*]quinoxaline (**27**). Yield: 30%.

6.1.3. General procedure for the synthesis of N-5-substituted 2-aryl-4,5-dihydro-1,2,4-triazolo[1,5-*a*]quinoxaline derivatives (2–15)

To a suspension of compounds **32**–**35**[26] (1.2 mmol) and small amounts of the corresponding 4,5-dehydro-derivatives **24**–**27** in anhydrous dichloromethane (40 mL) and anhydrous pyridine (0.1 mL) kept at 0 °C and under nitrogen atmosphere, a solution of the suitable acyl chloride or chloroformates (3.6 mmol) in anhydrous dichloromethane (4.0 mL) was drop by drop added. The reaction was stirred at 0 °C for 30 min (compounds **11**–**15**), at room temperature for 1 h (**4**–**5**, **7**, **9**–**10**), 4 h (compound **8**), otherwise at reflux for 3 h (**2**–**3**, **6**). After evaporation of the solvent at reduced pressure, the crude mixture was purified by silica gel column chromatography by using the suitable eluting system.

6.1.3.1. 1-(8-Chloro-2-phenyl-1,2,4-triazolo[1,5-*a*]quinoxalin-5(4*H*)-yl)-propan-1-one (2). Eluting system: chloroform/methanol 9.9:0.1. Yield: 25%; mp 142–144 °C (cyclohexane). ^1H NMR (DMSO-d_6) δ: 0.99 (t, 3H, CH_3, J = 7.33), 2.58 (q, 2H, CH_2, J = 7.33), 5.24 (s, 2H, CH_2), 7.43–7.53 (m, 4H, ar), 7.79–7.83 (m, 2H, ar), 8.09–8.13 (m, 2H, ar). IR: 1680. Anal. Calcd for ($C_{18}H_{15}ClN_4O$) C, 63.81; H, 4.46; N 16.54; Found: C, 63.24; H, 4.15; N, 17.02.

6.1.3.2. Ethyl 8-chloro-2-phenyl-1,2,4-triazolo[1,5-*a*]quinoxalin-5(4*H*)-carboxylate (3). Eluting system: chloroform/methanol 9.9:0.1. Yield: 48%; mp 177–179 °C (ethanol). ^1H NMR (DMSO-d_6) δ: 1.26 (t, 3H, CH_3, J = 6.96), 4.22 (q, 2H, CH_2, J = 6.96), 5.21 (s,

2H, CH_2), 7.42–7.58 (m, 4H, ar), 7.80–7.84 (m, 2H, ar), 8.07–8.13 (m, 2H, ar). IR: 1715. Anal. Calcd for ($C_{18}H_{15}ClN_4O_2$): C, 60.94; H, 4.26; N 15.79; Found: C, 61.78; H, 4.18; N, 16.06.

6.1.3.3. 1-(2-Phenyl-1,2,4-triazolo[1,5-*a*]quinoxalin-5(4*H*)-yl)-propan-1-one (4). Eluting system: cyclohexane/ethyl acetate/methanol 6:3.5:0.5. Yield: 28%; mp 126–128 °C (ethanol). ^{1}H NMR (DMSO-d_6) δ: 1.06 (t, 3H, CH_3, J = 7.29), 2.58 (q, 2H, CH_2, J = 7.29), 5.25 (s, 2H, CH_2), 7.40–7.53 (m, 5H, ar), 7.77 (d, 1H, ar, J = 6.73), 7.87 (d, 1H, ar, J = 7.40), 8.11 (d, 2H, ar, J = 6.73). IR: 1680. Anal. Calcd for ($C_{18}H_{16}N_4O$): C, 71.04; H, 5.30; N 18.41; Found: C, 71.37; H, 4.83; N, 18.07.

6.1.3.4. Methyl 2-phenyl-1,2,4-triazolo[1,5-*a*]quinoxalin-5(4*H*)-carboxylate (5). Eluting system: cyclohexane/ethyl acetate/methanol 8:3:0.15. Yield: 21%; mp 149–151 °C (methanol). ^{1}H NMR (DMSO-d_6) δ: 3.77 (s, 3H, OCH_3), 5.22 (s, 2H, CH_2), 7.40–7.47 (m, 2H, ar), 7.49–7.54 (m, 3H, ar), 7.79 (d, 1H, ar, J = 8.51), 7.86 (d, 1H, ar, J = 6.73), 8.11 (d, 2H, ar, J = 6.73). IR: 1700. Anal. Calcd for ($C_{17}H_{14}N_4O_2$): C, 66.66; H, 4.61; N 18.29; Found: C, 65.98; H, 4.33; N, 18.71.

6.1.3.5. Ethyl 2-phenyl-1,2,4-triazolo[1,5-*a*]quinoxalin-5(4*H*)-carboxylate (6). Eluting system: dichloromethane/methanol 9.8:0.2. Yield: 38%; mp 116–118 °C (methanol). ^{1}H NMR (DMSO-d_6) δ: 1.27 (t, 3H, CH_3, J = 6.96), 4.23 (q, 2H, CH_2, J = 6.96), 5.22 (s, 2H, CH_2), 7.40–7.47 (m, 2H, ar), 7.49–7.54 (m, 3H, ar), 7.80 (d, 1H, ar, J = 6.73), 7.85 (d, 1H, ar, J = 4.94), 8.11 (d, 2H, ar, J = 6.73). IR 1700. Anal. Calcd for ($C_{18}H_{16}N_4O_2$): C, 67.49; H, 5.03; N 17.49; Found: C, 68.93; H, 4.71; N, 17.94.

6.1.3.6. 1-(8-Methyl-2-phenyl-1,2,4-triazolo[1,5-*a*]quinoxalin-5(4*H*)-yl)-propan-1-one (7). Eluting system: chloroform/acetone 9:1. Yield 31%; mp 150–152 °C (cyclohexane). ^{1}H NMR (DMSO-d_6) δ: 0.98 (t, 3H, CH_3, J = 6.96), 2.43–2.57 (m, 5H, CH_2+-CH_3), 5.21 (s, 2H, CH_2), 7.20 (d, 1H, ar, J = 8.06), 7.49–7.52 (m, 3H, ar), 7.61–7.690(m, 2H, ar), 8.08–8.12 (m, 2H, ar). IR: 1670. Anal. Calcd for ($C_{19}H_{18}N_4O$): C, 71.68; H, 5.70; N 17.60; Found: C, 70.85; H, 5.51; N, 18.10.

6.1.3.7. Methyl 8-methyl-2-phenyl-1,2,4-triazolo[1,5-*a*]quinoxalin-5(4*H*)-carboxylate (8). Eluting system: dichloromethane/methanol 9.8:0.2. Yield: 12%; mp 132–134 °C (methanol). ^{1}H NMR (DMSO-d_6) δ: 2.40 (s, 3H, CH_3), 3.74 (s, 3H, OCH_3), 5.17 (s, 2H, CH_2), 7.18 (d, 1H, ar, J = 8.06), 7.49–7.52 (m, 3H, ar), 7.61–7.66 (m, 2H, ar), 8.07–8.11 (m, 2H, ar). IR: 1720. Anal. Calcd for ($C_{18}H_{16}N_4O_2$): C, 67.49; H, 5.03; N 17.49; Found: C, 68.15; H, 4.67; N, 17.95.

6.1.3.8. Ethyl 8-methyl-2-phenyl-1,2,4-triazolo[1,5-*a*]quinoxalin-5(4*H*)-carboxylate (9). Eluting system: dichloromethane/acetone/cyclohexane 8.8:0.7:0.5. Yield: 56%; mp 176–178 °C (ethyl acetate). ^{1}H NMR (DMSO-d_6) δ: 1.25 (t, 3H, CH_3, J = 6.96), 2.41 (s, 3H, CH_3), 4.19 (q, 2H, CH_2, J = 6.96), 5.18 (s, 2H, CH_2N), 7.19 (d, 1H, ar, J = 8.79), 7.50–7.53 (m, 3H, ar), 7.63–7.68 (m, 2H, ar), 8.08–8.12 (m, 2H, ar). IR: 1715. Anal. Calcd for ($C_{19}H_{18}N_4O_2$): C, 68.25; H, 5.43; N 16.76; Found: C, 68.77; H, 4.66; N, 16.12.

6.1.3.9. *n*-Propyl 8-methyl-2-phenyl-1,2,4-triazolo[1,5-*a*]quinoxalin-5(4*H*)-carboxylate (10). Eluting system: chloroform. Yield: 70%; mp 117–119 °C (ethanol). ^{1}H NMR (DMSO-d_6) δ: 0.90 (t, 3H, CH_3, J = 7.41), 1.58–1.69 (m, 2H, CH_2), 2.40 (s, 3H, CH_3), 4.10 (t, 2H, CH_2O, J = 6.23), 5.17 (s, 2H, CH_2N), 7.18 (d, 1H, ar, J = 8.42), 7.49–7.58 (m, 3H, ar), 7.62–7.66 (m, 2H, ar), 8.08–8.10 (m, 2H, ar). IR: 3070, 1725. Anal. Calcd for ($C_{20}H_{20}N_4O_2$): C, 68.95; H, 5.79; N 16.08; Found: C, 69.56; H, 5.47; N, 16.27.

6.1.3.10. 1-[2-(4-Methoxyphenyl)-8-methyl-1,2,4-triazolo[1,5-*a*]quinoxalin-5(4*H*)-yl]-propan-1-one (11). Eluting system: cyclohexane/ethyl acetate/methanol 9:2:1. Yield: 21%; mp 132–133 °C (cyclohexane); ^{1}H NMR (DMSO-d_6) δ: 1.00 (t, 3H, CH_3, J = 6.64), 2.44–2.53 (m, 5H, CH_2+CH_3), 3.83 (s, 3H, OCH_3), 5.20 (s, 2H, CH_2N), 7.08 (d, 2H, ar, J = 8.52), 7.20 (d, 1H, ar, J = 8.32), 7.63 (d, 1H, ar, J = 7.60), 7.68 (s, 1H, ar), 8.03 (d, 2H, ar, J = 8.52). Anal. Calcd for ($C_{20}H_{20}N_4O_2$): C, 68.95; H, 5.79; N 16.08; Found: C, 68.13; H, 5.99; N, 15.83.

6.1.3.11. Ethyl 2-(4-methoxyphenyl)-8-methyl-1,2,4-triazolo[1,5-*a*]quinoxalin-5(4*H*)-carboxylate (12). Eluting system: dichloromethane/cyclohexane/ethylacetate 9:0.5:0.5. Yield: 21%; mp 141–142 °C (cyclohexane); ^{1}H NMR (DMSO-d_6) δ: 1.26 (t, 3H, CH_3, J = 7.08), 2.42 (s, 3H, CH_3), 3.84 (s, 3H, OCH_3), 4.19 (q, 2H, CH_2, J = 7.08), 5.17 (s, 2H, CH_2), 7.08 (d, 2H, ar, J = 8.76), 7.19 (d, 1H, ar, J = 8.40), 7.65–7.67 (m, 2H, ar), 8.03 (d, 2H, ar, J = 8.76). IR: 1708. Anal. Calcd for ($C_{20}H_{20}N_4O_3$): C, 65.92; H, 5.53; N 15.38; Found: C, 66.66; H, 5.78; N, 14.87.

6.1.3.12. Propyn-2-yl 2-(4-methoxyphenyl)-8-methyl-1,2,4-triazolo[1,5-*a*]quinoxalin-5(4*H*)-carboxylate (13). Eluting system: cyclohexane/ethyl acetate 6:4. Yield 21%. mp 134–135 °C (cyclohexane); ^{1}H NMR (DMSO-d_6) δ: 2.42 (s, 3H, CH_3), 3.63 (s, 1H, CCH), 3.84 (s, 3H, OCH_3), 4.84 (s, 2H, OCH_2), 5.18 (s, 2H, NCH_2), 7.09 (d, 2H, ar, J = 8.40), 7.21 (d, 1H, ar, J = 7.68), 7.62 (d, 1H, ar, J = 7.68), 7.68 (s, 1H, ar), 8.04 (d, 2H, ar, J = 8.48). IR: 3260, 1721. Anal. Calcd for ($C_{21}H_{18}N_4O_3$): C, 67.37; H, 4.85; N 14.96; Found: C, 67.97; H, 4.05; N, 15.13.

6.1.3.13. 2-Phenyl-1-[2-(4-methoxyphenyl)-8-methyl-1,2,4-triazolo[1,5-*a*]quinoxalin-5(4*H*)-yl)-ethanone (14). Eluting system: dichloromethane/acetone 9:1. Yield: 22%; mp 188–190 °C (cyclohexane); ^{1}H NMR (DMSO-d_6) δ: 2.44 (s, 3H, CH_3), 3.84 (s, 3H, OCH_3), 3.96 (s, 2H, $COCH_2$), 5.22 (s, 2H, CH_2N), 7.08 (d, 2H, ar, J = 7.12), 7.10–7.23 (m, 6H, ar), 7.66–7.70 (m, 2H, ar), 8.03 (d, 2H, ar, J = 7.12). IR: 1662. Anal. Calcd for ($C_{25}H_{22}N_4O_2$): C, 73.15; H, 5.40; N 13.65; Found: C, 72.54; H, 5.63; N, 14.15.

6.1.3.14. Benzyl 2-(4-methoxyphenyl)-8-methyl-1,2,4-triazolo[1,5-*a*]quinoxalin-5(4*H*)-carboxylate (15). Eluting system: cyclohexane/ethyl acetate 6:4. Yield: 31%, mp 119–120 °C (cyclohexane); ^{1}H NMR (DMSO-d_6) δ: 2.40 (s, 3H, CH_3), 3.83 (s, 3H, OCH_3), 5.19 (s, 2H, OCH_2), 5.23 (s, 2H, NCH_2), 7.10 (d, 2H, ar, J = 8.61), 7.17 (d, 1H, ar, J = 8.24), 7.35–7.45 (m, 5H, ar), 7.66 (m, 2H, ar), 8.03 (d, 2H, ar, J = 8.60). IR: 1722. Anal. Calcd for ($C_{25}H_{22}N_4O_3$): C, 70.41; H, 5.20; N 13.14; Found: C, 70.59; H, 4.66; N, 13.91.

6.1.4. 3-(4-Methoxyphenyl)-1-(5-methyl-2-nitrophenyl)-1,2,4-triazole-5-chloromethyl (37)

To a solution of chloroacetyl chloride (3.4 mmol) in anhydrous toluene (15 mL) at 80 °C, the amidrazone **36**[18] (1.7 mmol) was added portion by portion. The reaction mixture was heated at reflux for 3 h. Then, the solvent was removed under reduced pressure and the oily residue was worked up with a mixture of ethyl acetate/petroleum ether 1:1. The solid which separated was collected by filtration and washed with petroleum ether. Yield: 72%; mp 127–128 °C (ethanol); ^{1}H NMR (DMSO-d_6) δ: 2.51 (s, 3H, CH_3), 3.82 (s, 3H, OCH_3), 4.95 (s, 2H, CH_2), 7.07 (d, 2H, ar, J = 8.88), 7.72 (d, 1H, ar, J = 8.32), 7.81(s, 1H, ar), 7.93 (d, 2H, ar, J = 8.88), 8.23 (d, 1H, ar, J = 8.40). Anal. Calcd for ($C_{17}H_{15}Cl\ N_4O_3$): C, 56.91; H, 4.21; N 15.66; Found: C, 57.27; H, 4.10; N, 16.09.

6.1.5. 2-(4-Methoxyphenyl)-8-methyl-4,5-dihydro-1,2,4-triazolo[1,5-*a*]quinoxaline (35)

To a solution of the 5-chloromethyl-1,2,4-triazole derivative **37** (1.59 mmol) in ethanol (75 mL), an excess of $SnCl_2$ dihydrate (4.77 mmol) was added under nitrogen atmosphere. Then, the reaction mixture was heated at reflux, under nitrogen atmosphere, for 40 h. After evaporation of the solvent at reduced pressure, the resulting solid was worked up with diethyl ether, collected by filtration and washed with a large amount of water. The crude product, containing a small amount of the dehydro-derivative **27** (**27/35**, ratio 1:10, ^{1}H NMR evaluation) was used as it is for the next step. Yield: 83%.

6.1.6. 3-(4-Methoxyphenyl)-1-(5-methyl-2-nitrophenyl)-1,2,4-triazole (38)

To a suspension of the amidrazone **36**[18] (1.0 mmol) in ethyl orthoformate (1.25 mL), *p*-toluenesulfonic acid (10 mg) was added. The reaction mixture was heated at 100 °C for 30 min. Upon cooling, a orange solid precipitated which was collected by filtration and washed with diethyl ether. Yield 54%; mp 138–139 °C (ethanol); ^{1}H NMR (DMSO-d_6) δ: 2.50 (s, 3H, CH_3), 3.82 (s, 3H, OCH_3), 7.06 (d, 2H, ar, J = 8.76), 7.60 (d, 1H, ar, J = 8.36), 7.80 (s, 1H, ar), 7.94 (d, 2H, ar, J = 8.70), 8.09 (d, 1H, ar, J = 8.36), 9.09 (s, 1H, CH). Anal. Calcd for ($C_{16}H_{14}N_4O_3$): C, 61.93; H, 4.55; N 18.06; Found: C, 61.13; H, 4.89; N, 18.72.

6.1.7. 2-[3-(4-Methoxyphenyl)-1,2,4-triazol-1-yl]-4-methylphenylamine (39)

To a solution of the 2-nitrophenyl-1,2,4-triazole derivative **38** (2.0 mmol) in ethyl acetate (50 mL), the catalyst (10% Pd/C, 50 mg) was added. Hydrogenation of the resulting mixture was performed at 30 Psi until disappearance of the starting material (TLC monitoring, eluting system cyclohexane/ethyl acetate 6:4). The catalyst was removed by filtration and the solvent was distilled under reduced pressure to yield a solid. Yield 69%; mp 131–132 °C (ethanol); ^{1}H NMR (DMSO-d_6) δ: 2.22 (s, 3H, CH_3), 3.82 (s, 3H, OCH_3), 5.31 (s, 2H, NH_2), 6.84 (d, 1H, ar, J = 8.24), 7.02 (d, 1H, ar, J = 8.20), 7.06 (d, 2H, ar, J = 8.80), 7.14 (s, 1H, ar), 8.02 (d, 2H, ar, J = 8.76), 8.83 (s, 1H, CH). IR: 3448, 3348 Anal. Calcd for ($C_{16}H_{16}N_4O$): C, 68.55; H, 5.75; N 19.99; Found: C, 67.71; H, 5.05; N, 20.17.

6.1.8. General procedure for the synthesis of 2-[3-(4-methoxyphenyl)-1,2,4-triazol-1-yl]-4-methylphenylcarbamates (16–19)

A solution of the suitable chloroformates (compounds **16**–**17**, **19**) (3.2 mmol) or phenacetyl chloride (**18**) (3.2 mmol) in anhydrous dichloromethane (3.2 mL) was drop by drop added to a solution of the triazole derivative **39** (1.07 mmol) in anhydrous dichloromethane (32 mL) and anhydrous pyridine (0.05 mL) at 0 °C. The reaction mixture was kept at 0 °C for 2 h. Then, the solvent was removed under reduced pressure and the solid was worked up with water (20 mL), collected and washed with water (compounds **16**–**17**, **19**). Otherwise (compound **18**), the solid was worked up with 10% aqueous solution of $NaHCO_3$ (20 mL), and the resulting mixture extracted with ethyl acetate (15 mL × 3). The organic layers were washed with water (20 mL), anhydrified (Na_2SO_4) and evaporated under reduced pressure to give a yellow solid.

6.1.8.1. Ethyl 2-[3-(4-methoxyphenyl)-1*H*-1,2,4-triazol-1-yl]-4-methylphenylcarbamate (16).

Yield: 85%; mp 117–118 °C (cyclohexane); ^{1}H NMR (DMSO-d_6) δ: 1.12 (t, 3H, CH_3, J = 7.08), 2.37 (s, 3H, CH_3), 3.83 (s, 3H, OCH_3), 4.03 (q, 2H, CH_2, J = 7.08), 7.07 (d, 2H, ar, J = 8.88), 7.30 (d, 1H, ar, J = 8.41), 7.45 (s, 1H, ar), 7.58 (d, 1H, ar, J = 8.16), 8.00 (d, 2H, ar, J = 8.84), 8.84 (s, 1H, CH), 9.13 (s, 1H, NH). IR: 1726. Anal. Calcd for. ($C_{19}H_{20}N_4O_3$): C, 64.76; H, 5.72; N 15.90; Found: C, 64.66; H, 5.01; N, 16.18.

6.1.8.2. Propyn-2-yl 2-[3-(4-methoxyphenyl)-1*H*-1,2,4-triazol-1-yl]-4-methylphenylcarbamate (17).

Yield: 54%; mp 132–133 °C (cyclohexane); ^{1}H NMR (DMSO-d_6) δ: 2.37 (s, 3H, CH_3), 3.53 (s, 1H, CH), 3.83 (s, 3H, OCH_3), 4.68 (s, 2H, CH_2), 7.07 (d, 2H, ar, J = 8.88), 7.32 (d, 1H, ar, J = 8.28), 7.46 (s, 1H, ar), 7.59 (d, 1H, ar, J = 8.04), 8.01 (d, 2H, ar, J = 8.90), 8.84 (s, 1H, CH), 9.37 (s, 1H, NH). IR: 1720. Anal. Calcd for ($C_{20}H_{18}N_4O_3$): C, 66.29; H, 5.01; N 15.46; Found: C, 66.76; H, 4.55; N, 14.93.

6.1.8.3. *N*-[2-(3-(4-methoxyphenyl)-1*H*-1,2,4-triazol-1-yl)-4-methylphenyl]-2-phenylacetamide (18).

Yield: 76%; mp 138–139 °C (ethanol); ^{1}H NMR (DMSO-d_6) δ: 2.36 (s, 3H, CH_3), 3.59 (s, 2H, CH_2), 3.84 (s, 3H, OCH_3), 7.09 (d, 2H, ar, J = 8.80), 7.19 (s, 5H, ar), 7.30 (d, 1H, ar, J = 8.44), 7.43 (s, 1H, ar), 7.71 (d, 1H, ar, J = 8.32), 8.01 (d, 2H, ar, J = 8.80), 8.50 (s, 1H, CH), 9.72 (s, 1H, NH). IR: 3247, 3096, 1688. Anal. Calcd for ($C_{24}H_{22}N_4O_2$): C, 72.34; H, 5.57; N 14.06; Found: C, 73.05; H, 5.74; N, 14.54.

6.1.8.4. Benzyl 2-[3-(4-methoxyphenyl)-1*H*-1,2,4-triazol-1-yl]-4-methylphenylcarbamate (19).

Yield: 34%; mp 149–150 °C (ethanol); ^{1}H NMR (DMSO-d_6) δ: 2.37 (s, 3H, CH_3), 3.83 (s, 3H, OCH_3), 5.06 (s, 2H, CH_2), 7.06 (d, 2H, ar, J = 8.68), 7.31 (s, 6H, ar), 7.46 (s, 1H, ar), 7.61 (d, 1H, ar, J = 8.08), 8.00 (d, 2H, ar, J = 8.61), 8.85 (s, 1H, CH), 9.34 (s, 1H, NH). IR: 3227, 3109, 1728. Anal. Calcd for ($C_{24}H_{22}N_4O_3$): C, 69.55; H, 5.35; N 13.52; Found: C, 68.88; H, 4.95; N, 14.18.

6.1.9. N^1-Phenyl-N^2-(4-methoxybenzoyl)-hydrazide (40)[27,28]

To a mixture of phenylhydrazine (9.25 mmol) in anhydrous pyridine (10 mL) a solution of equimolar amount of *p*-anisoyl chloride in anhydrous pyridine (5 mL) was drop by drop added. The reaction mixture was heated at reflux for 5 h. The excess of pyridine was removed by distillation under reduced pressure. The residue was treated with HCl 2 M solution (30 mL) and the resulting solid was collected by filtration and well washed with water. Yield: 75%; mp 165–168 °C (ethanol) (lit. Mp 177–178 °C).[28]

6.1.10. N^1-Phenyl-N^2-[α-chloro-(4-methoxybenzyliden)] hydrazine (41)[29]

A suspension of equimolar amount of hydrazide **40**[27,28] (4.13 mmol) and PCl_5 in $POCl_3$ (7 mL) was heated at reflux for 4 h. Then, another portion (4.13 mmol) of PCl_5 was added and the heating continued for 2 h. Evaporation at reduced pressure of the excess of $POCl_3$ gave an oily residue which was treated with cold water (50 mL) and quickly collected. The compound was used as it is without further purification. Yield: 90%; mp 117–121 °C (lit. mp 119–120 °C). ^{1}H NMR ($CDCl_3$) δ: 3.89 (s, 3H, OCH_3), 6.98 (d, 2H, ar, J = 8.60), 7.33–7.35 (m, 1H, ar), 7.38–7.46 (m, 4H, ar), 8.06 (d, 2H, ar, J = 8.61).

6.1.11. 3-(4-Methoxyphenyl)-1-phenyl-1*H*-1,2,4-triazol-5-amine (42)

A mixture of the chloro-derivative **41**[29] (4.12 mmol) and an excess of cyanamide (20.6 mmol) was heated at 100 °C for 20 min. The crude mass was worked up with ethyl acetate (20 mL) and the resulting solid was filtered off and well washed with ethyl acetate. The mother liquors were evaporated under reduced pressure to yield a solid which was purified by silica gel column chromatography, eluting system: dichloromethane/methanol 9:1, and then dichloromethane/ethyl acetate 8:2. Yield: 45%; mp 152–155 °C (toluene). ^{1}H NMR (DMSO-d_6) δ: 3.80 (s, 3H, OCH_3), 6.51 (br s, 2H, NH_2), 7.01 (d, 2H, ar, J = 8.68), 7.39 (t, 1H,

ar, J = 7.28), 7.54 (t, 2H, ar, J = 7.64), 7.62 (d, 2H, ar, J = 7.88), 7.88 (d, 2H, ar, J = 8.60). IR: 3303. Anal. Calcd for ($C_{15}H_{14}N_4O$): C, 67.65; H, 5.30; N 21.04; Found: C, 67.93; H, 4.87; N, 21.27.

6.1.12. *N*-Acetyl-*N*-[3-(4-methoxyphenyl)-1-phenyl-1*H*-1,2,4-triazol-5-yl]acetamide (20)

A mixture of the triazole **42** (0.75 mmol) and acetic anhydride (2.25 mmol) in anhydrous pyridine (3 mL) was heated at reflux for 8 h. The crude mass was worked up with water and the resulting solid collected by filtration ad purified by silica gel column chromatography, eluting system dichloromethane/ethyl acetate 8:2. Yield: 38%; mp 130–132 °C (cyclohexane/ethyl acetate 8:2); ^{1}H NMR (DMSO-d_6) δ: 2.29 (2, 6H, 2CH_3), 3.83 (s, 3H, OCH_3), 7.09 (d, 2H, ar, J = 8.64), 7.54–7.60 (m, 5H, ar), 8.01 (d, 2H, ar, J = 8.64). IR: 1749, 1715. Anal. Calcd for ($C_{19}H_{18}N_4O_3$): C, 65.13; H, 5.18; N 15.99; Found: C, 64.66; H, 5.45; N, 16.35.

6.1.13. General procedure for the synthesis of *N*-[3-(4-methoxyphenyl)1-phenyl-1*H*-1,2,4-triazol-5-yl]benzamide (21) and *N*-benzoyl-*N*-[3-(4-methoxyphenyl)-1-phenyl-1*H*-1,2,4-triazol-5-yl]benzamide (22)

A solution of a little excess of benzoyl chloride (0.54 mmol) in anhydrous tetrahydrofuran (2 mL) was drop by drop added to a solution of the 1,2,4-triazol-5-amino derivative **42** (0.45 mmol) in anhydrous tetrahydrofuran (8 mL) and anhydrous pyridine (3 mL). The reaction mixture was heated at reflux for 25 h. After 10 h, another portion (0.5 mmol) of benzoyl chloride was added. After cooling, water (30 mL) and ice (20 g) were added and the resulting solution was extracted with ethyl acetate (30 mL × 4). The organic layers were washed with water (30 mL × 4), with a saturated solution of $NaHCO_3$ (30 mL), and again with water (40 mL), then anhydrified (Na_2SO_4) and evaporated under reduced pressure. The resulting oily residue was purified by silica gel column chromatography, eluting system dichloromethane/ethyl acetate 1:1.

6.1.13.1. Compound (21). Yield: 20%; mp 156–158 °C (diethyl ether/petroleum ether); ^{1}H NMR (DMSO-d_6) δ: 3.84 (s, 3H, OCH_3), 7.08 (d, 2H, ar, J = 8.44), 7.42 (t, 1H, ar, J = 6.88), 7.50–7.56 (m, 4H, ar), 7.65 (d, 3H, ar, J = 7.16), 7.91 (d, 2H, ar, J = 7.40), 8.01 (d, 2H, ar, J = 8.36), 11.17 (s, br, 1H, NH). IR: 3194, 1667. Anal. Calcd for ($C_{22}H_{18}N_4O_2$): C, 71.34; H, 4.90; N 15.13; Found: C, 70.67; H, 5.30; N, 14.59.

6.1.13.2. Compound (22). Yield: 60%; mp 154–156 °C (ethanol); ^{1}H NMR (DMSO-d_6) δ: 3.82 (s, 3H, OCH_3), 7.05 (d, 2H, ar, J = 6.88), 7.41–7.45 (m, 6H, ar), 7.50–7.55 (m, 3H, ar), 7.59 (t, 2H, ar, J = 7.48), 7.63 (d, 4H, ar, J = 7.12), 7.93 (d, 2H, ar, J = 4.88). IR: 1708. Anal. Calcd for. ($C_{29}H_{22}N_4O_3$): C, 73.40; H, 4.67; N 11.81; Found: C, 73.01; H, 5.10; N, 11.12.

6.1.14. 1-[3-(4-Methoxyphenyl)-1-phenyl-1*H*-1,2,4-triazol-5-yl]-3-phenylurea (23)

A solution of phenylisocyanate (0.26 mmol) in anhydrous dichloromethane (4 mL) was drop by drop added to an equimolar amount of the 5-aminotriazole **42** in anhydrous dichloromethane (4 mL) maintained at 5 °C. The reaction mixture was then kept at room temperature for 20 days. The solvent was removed until small volume and the resulting solid was collected. Yield 42%; mp 202–204 °C (2-methoxyethanol); ^{1}H NMR (DMSO-d_6) δ: 3.83 (s, 3H, OCH_3), 7.02 (t, 1H, ar, J = 7.20), 7.07 (d, 2H, ar, J = 8.44), 7.30 (t, 2H, ar, J = 7.25), 7.44–7.49 (m, 3H, ar), 7.57 (t, 2H, ar, J = 7.44), 7.66 (d, 2H, ar, J = 7.84), 7.99 (d, 2H, ar, J = 8.32), 9.43 (s, 1H, NH), 9.75 (s, 1H, NH). IR: 3182, 3145, 1685. Anal. Calcd for ($C_{22}H_{19}N_5O_2$): C, 68.56; H, 4.97; N 18.17; Found: C, 69.07; H, 5.31; N, 18.44.

6.2. Computational methodologies

All molecular modeling studies were performed on a 2 CPU (PIV 2.0–3.0 GHZ) Linux PC. Homology modeling, energy minimization, and docking studies were carried out using Molecular Operating Environment (MOE, version 2010.10) suite.[35] Manual docking and Monte Carlo studies of the MRS 1220 binding mode were done using MOE and Schrodinger Macromodel (ver. 8.0)[42] with Schrodinger Maestro interface. Compounds docking analyses were then performed with MOE. All ligand structures were optimized using RHF/AM1 semiempirical calculations and the software package MOPAC implemented in MOE was utilized for these calculations.[37]

6.2.1. Homology modeling of the human A_3AR

Homology models of the hA_3AR were built using recently solved X-ray structures of the antagonist-bound hA_{2A} AR as templates (pdb code: 3EML; 2.6-Å resolution;[30] pdb code: 3PWH; 3.3-Å resolution;[31] pdb code: 3REY; 3.3-Å resolution;[31] pdb code: 3UZA; 3.3-Å resolution[32]). A multiple alignment of the AR primary sequences was built within MOE as preliminary step. For all hA_3AR models, the boundaries identified from the used X-ray crystal structure of hA_{2A} AR were then applied for the corresponding sequences of the TM helices of the hA_3AR. The missing loop domains were built by the loop search method implemented in MOE. Once the heavy atoms were modeled, all hydrogen atoms were added, and the protein coordinates were then minimized with MOE using the AMBER99 force field.[43] The minimizations were performed by 1000 steps of steepest descent followed by conjugate gradient minimization until the RMS gradient of the potential energy was less than 0.05 kJ mol^{-1} Å^{-1}. The reliability and quality of these models were checked using the Protein Geometry Monitor application within MOE, which provides a variety of stereochemical measurements for inspection of the structural quality in a given protein, like backbone bond lengths, angles and dihedrals, Ramachandran φ–ψ dihedral plots, and sidechain rotamer and non-bonded contact quality.

6.2.2. Preliminary docking analysis with MRS 1220

A preliminary docking analysis was performed by manually docking MRS 1220 structure within each hA_3AR model binding site. The obtained hA_3AR–MRS 1220 complexes were then subjected to energy minimization refinement and to Monte Carlo analysis to explore the favorable binding conformations. This analysis was conducted by Monte Carlo Conformational Search protocol implemented in Schrodinger Macromodel. The input structure consisted of the ligand and a shell of receptor amino acids within the specified distance (6 Å) from the ligand. A second external shell of all the residues within a distance of 8 Å from the first shell was kept fixed. During the Monte Carlo conformational searching, the input structure was modified by random changes in user-specified torsion angles (for all input structure residues), and molecular position (for the ligand). Hence, the ligand was left free to be continuously re-oriented within the binding site and the conformation of both ligand and internal shell residues could be explored and reciprocally relaxed. The method consisted of 10,000 Conformational Search steps with MMFF94s force field.[44–50] For each A_{2A}AR-based model, the best hA_3AR–MRS 1220 complex was saved. The four final complexes served as input in MOE and were subjected to energy minimization with the same protocol as above. This protocol was recently used to prepare hA_3AR models for docking and dynamics studies of nucleoside agonists at the same receptor.[41,51]

6.2.3. Molecular docking analysis

All compound structures were docked into the binding site of the four hA_3AR models using the MOE Dock tool. This method is

divided into a number of stages: *Conformational Analysis of ligands*. The algorithm generated conformations from a single 3D conformation by conducting a systematic search. In this way, all combinations of angles were created for each ligand. *Placement*. A collection of poses was generated from the pool of ligand conformations using Triangle Matcher placement method. Poses were generated by superposition of ligand atom triplets and triplet points in the receptor binding site. The receptor site points are alpha sphere centers which represent locations of tight packing. At each iteration a random conformation was selected, a random triplet of ligand atoms and a random triplet of alpha sphere centers were used to determine the pose. *Scoring*. Poses generated by the placement methodology were scored using two available methods implemented in MOE, the *London dG* scoring function which estimates the free energy of binding of the ligand from a given pose, and *Affinity dG* scoring which estimates the enthalpic contribution to the free energy of binding. The top 30 poses for each ligand were output in a MOE database.

6.2.4. Post docking analysis

The five top-score docking poses of each compound were then subjected to AMBER99 force field energy minimization until the RMS gradient of the potential energy was less than 0.05 kJ mol^{-1} $Å^{-1}$. Receptor residues within 6 Å distance from the ligand were left free to move, while the remaining receptor coordinates were kept fixed. AMBER99 partial charges of receptor and MOPAC output partial charges of ligands were utilized. Once the compound-binding site energy minimization was completed, receptor coordinates were fixed and a second energy minimization stage was performed leaving only compound atoms free to move. MMFF94 force field was applied. For each compound, the minimized docking poses were then rescored using *London dG* and *Affinity dG* scoring functions and the *dock-pK_i* predictor. The latter tool estimates the pK_i for each ligand using the 'scoring.svl' script retrievable at the SVL exchange service (Chemical Computing Group, Inc. SVL exchange: http://svl.chemcomp.com). The algorithm is based on an empirical scoring function consisting of a directional hydrogen-bonding term, a directional hydrophobic interaction term, and an entropic term (ligand rotatable bonds immobilized in binding). The four top-score docking poses according to at least two out of three scoring functions were selected for final ligand-target interaction analysis for each compound.

6.3. Pharmacology

6.3.1. Human cloned A_1, A_{2A}, and A_3 AR Binding Assay

Binding experiments at hA_1 and hA_{2A} ARs, stably expressed in CHO cells, were performed as previously described,[52] using [^{3}H]DPCPX and [^{3}H]NECA, respectively, as radioligands. Displacement of [^{125}I]AB-MECA from hA_3 AR, stably expressed in CHO cells, was performed as reported in Ref. 53.

6.3.2. A_{2B} AR functional assay

Intracellular cyclic AMP (cAMP) levels were measured using a competitive protein binding method.[54] CHO cells, expressing recombinant human A_{2B}ARs, were harvested by trypsinization. After centrifugation and re-suspension in medium, cells (~30,000) were plated in 24-well plates in 0.5 mL of medium. After 24 h, the medium was removed, and the cells were incubated at 37 °C for 15 min with 0.5 mL of Dulbecco's Modified Eagle Medium (DMEM) in the presence of adenosine deaminase (ADA) (1 U/mL) and the phosphodiesterase inhibitor Ro20-1724 (20 μM). The pharmacological profile of the compounds towards A_{2B} ARs was evaluated by assessing cAMP accumulation in the absence or presence of the agonist NECA (100 nM). Cells were incubated in the reaction medium (15 min at 37 °C) with the target compounds (10 μM) and then were treated with the agonist.

Following incubation, the reaction was terminated by the removal of the medium and the addition of 0.4 N HCl. After 30 min, lysates were neutralized with 4 N KOH, and the suspension was centrifuged at 800 g for 5 min. For the determination of cAMP production, bovine adrenal cAMP binding protein was incubated with [^{3}H]cAMP (2 nM) and 50 μL of cell lysate or cAMP standard (0–160 pmol) at 0 °C for 150 min in a total volume of 300 μL. Bound radioactivity was separated by rapid filtration through GF/C glass fiber filters and washed twice with 4 mL 50 mM Tris–HCl, pH 7.4. The radioactivity was measured by liquid scintillation spectrometry.

6.3.3. Data analysis

The concentration of the tested compounds that produced 50% inhibition of specific [^{3}H]DPCPX, [^{3}H]NECA, [^{125}I]AB-MECA, [^{3}H]CHA and [^{3}H]CGS 21680 binding (IC_{50}) was calculated using a non-linear regression method implemented by the InPlot program (Graph-Pad, San Diego, CA, U.S.A.) with five concentrations of displacer, each performed in triplicate. Inhibition constants (K_i) were calculated according to the Cheng–Prusoff equation.[55] The K_d values of [^{3}H]DPCPX, [^{3}H]NECA and [^{125}I]AB-MECA in hA_1, hA_{2A} and hA_3 ARs in CHO cell membranes were 3 nM, 30 nM and 1.4 nM, respectively. The dissociation constant (K_d) of [^{3}H]CHA and [^{3}H]CGS 21680 in cortical and striatal bovine brain membranes were 1.2 and 14 nM, respectively.

Acknowledgment

This work was supported by a Grant from the Italian Ministry for University and Research (MIUR, FIRB RBNE03YA3L project).

References and notes

1. Fredholm, B. B.; IJzerman, A. P.; Jacobson, K. A.; Linden, J.; Muller, C. E. *Pharmacol. Rev.* **2011**, *63*, 1.
2. Meyerhof, W.; Muller-Brechlin, R.; Richter, D. *FEBS Lett.* **1991**, *284*, 155.
3. Salvatore, C. A.; Jacobson, K. A.; Taylor, H. E.; Linden, J.; Johnson, R. G. *Proc. Natl. Acad. Sci. U.S.A.* **1993**, *90*, 10365.
4. Fredholm, B. B.; IJzerman, A. P.; Jacobson, K. A.; Klotz, K. N.; Linden, J. *Pharmacol. Rev.* **2001**, *53*, 527.
5. Linden, J. *Trends Pharmacol. Sci.* **1994**, *15*, 298.
6. Schulte, G.; Fredholm, B. B. *Cell Signalling* **2003**, *15*, 813.
7. Mozzicato, S.; Joshi, B. V.; Jacobson, K. A.; Liang, B. T. *FASEB J.* **2004**, *18*, 406.
8. Shneyvays, V. D.; Leshem; Zinman, T.; Mamedova, L. K.; Shainberg, K. A.; Jacobson, A. *Am. J. Physiol. Heart Circ. Physiol.* **2005**, *288*, H279.
9. Cheong, S. L.; Federico, S.; Venkatesan, G.; Mandel, A. L.; Shao, Y.-M.; Moro, S.; Spalluto, G.; Pastorin, G. *Med. Chem. Rev.* **2013**, *33*, 235.
10. Pugliese, A. M.; Coppi, E.; Volpini, R.; Cristalli, G.; Corradetti, R.; Jeong, L. S.; Jacobson, K. A.; Pedata, F. *Biochem. Pharmacol.* **2007**, *74*, 768.
11. Colotta, V.; Catarzi, D.; Varano, F.; Capelli, F.; Lenzi, O.; Filacchioni, G.; Martini, C.; Trincavelli, L.; Ciampi, O.; Pugliese, A. M.; Pedata, F.; Schiesaro, A.; Morizzo, E.; Moro, S. *J. Med. Chem.* **2007**, *50*, 4061.
12. Merighi, S.; Benini, A.; Mirandola, P.; Gessi, S.; Varani, K.; Leung, E.; Maclennan, S.; Borea, P. A. *Biochem. Pharmacol.* **2006**, *72*, 19.
13. Gessi, S.; Cattabriga, E.; Avitabile, A.; Gafa', R.; Lanza, G.; Cavazzini, L.; Bianchi, N.; Gambari, R.; Feo, C.; Liboni, A.; Gullini, S.; Leung, E.; Mac-Lennan, S.; Borea, P. A. *Clin. Cancer Res.* **2004**, *10*, 5895.
14. Gessi, S.; Merighi, S.; Varani, K.; Leung, E.; Mac Lennan, S.; Borea, P. A. *Pharmacol. Ther.* **2008**, *117*, 123.
15. Colotta, V.; Cecchi, L.; Catarzi, D.; Filacchioni, G.; Martini, C.; Tacchi, P.; Lucacchini, A. *Eur. J. Med. Chem.* **1995**, *30*, 133.
16. Catarzi, D.; Colotta, V.; Varano, F.; Filacchioni, G.; Martini, C.; Trincavelli, L.; Lucacchini, A. *Il Farmaco.* **2004**, *59*, 71.
17. Catarzi, D.; Colotta, V.; Varano, F.; Calabri, F. R.; Lenzi, O.; Filacchioni, G.; Trincavelli, L.; Martini, C.; Tralli, A.; Monopoli, C.; Moro, S. *Bioorg. Med. Chem.* **2005**, *13*, 705.
18. Catarzi, D.; Colotta, V.; Varano, F.; Lenzi, O.; Filacchioni, G.; Trincavelli, L.; Martini, C.; Monopoli, C.; Moro, S. *J. Med. Chem.* **2005**, *48*, 7932.
19. Francis, J. E.; Cash, W. D.; Psychoyos, S.; Ghai, G.; Wenk, P.; Friedmann, R. C.; Atkins, C.; Warren, V.; Furness, P.; Hyun, J. L. *J. Med. Chem.* **1988**, *31*, 1014.
20. Jung, K. Y.; Kim, S. K.; Gao, Z. G.; Gross, A. S.; Melman, N.; Jacobson, K. A.; Kim, Y. C. *Bioorg. Med. Chem.* **2004**, *12*, 613.

21. Alanine, A.; Anselm, L.; Steward, L.; Thomi, S.; Vifian, W.; Groaning, M. D. *Bioorg. Med. Chem. Lett.* **2004**, *14*, 817.
22. Cosimelli, B.; Greco, G.; Ehlardo, M.; Novellino, E.; Da Settimo, F.; Taliani, S.; La Motta, C.; Bellandi, M.; Tuccinardi, T.; Martinelli, A.; Ciampi, O.; Trincavelli, M. L.; Martini, C. *J. Med. Chem.* **2008**, *51*, 1764.
23. Carlsson, J.; Tosh, D. K.; Phan, K.; Gao, Z.-G.; Jacobson, K. A. *Med. Chem. Lett.* **2012**, *3*, 715.
24. Catarzi, D.; Colotta, V.; Varano, F.; Poli, D.; Squarcialupi, L.; Filacchioni, G.; Varani, K.; Vincenzi, F.; Borea, P. A.; Dal Ben, D.; Lambertucci, C.; Cristalli, G. *Bioorg. Med. Chem.* **2013**, *21*, 283.
25. Morizzo, E.; Capelli, F.; Lenzi, O.; Catarzi, D.; Varano, F.; Filacchioni, G.; Vincenzi, F.; Varani, K.; Borea, P. A.; Colotta, V.; Moro, S. *J. Med. Chem.* **2007**, *50*, 6596.
26. Catarzi, D.; Cecchi, L.; Colotta, V.; Melani, F.; Filacchioni, G.; Martini, C.; Giusti, L.; Lucacchini, A. *Il Farmaco.* **1993**, *48*, 1065.
27. Zhang, C.-Y.; Liu, X.-H.; Wang, B.-L.; Wang, S. H.; Li, Z.-M. *Chem. Biol. Drug Des.* **2010**, *75*, 489.
28. Baumstark, A. L.; Vasquez, P. C. *J. Org. Chem.* **1983**, *48*, 65.
29. Gelleri, A.; Messmer, A.; Pinter, I.; Radics, L. *J. Prakt. Chem.* **1976**, *318*, 881.
30. Jaakola, V. P.; Ijzerman, A. P. *Curr. Opin. Struct. Biol.* **2010**, *20*, 401.
31. Doré, A. S.; Robertson, N.; Errey, J. C.; Ng, I.; Hollenstein, K.; Tehan, B.; Hurrell, E.; Bennett, K.; Congreve, M.; Magnani, F.; Tate, C. G.; Weir, M.; Marshall, F. H. *Structure* **2011**, *19*, 1283.
32. Congreve, M.; Andrews, S. P.; Dore, A. S.; Hollenstein, K.; Hurrell, E.; Langmead, C. J.; Mason, J. S.; Ng, I. W.; Tehan, B.; Zhukov, A.; Weir, M.; Marshall, F. H. *J. Med. Chem.* **1898**, *2012*, 55.
33. Dal Ben, D.; Lambertucci, C.; Marucci, G.; Volpini, R.; Cristalli, G. *Curr. Top. Med. Chem.* **2010**, *10*, 993.
34. Costanzi, S.; Ivanov, A. A.; Tikhonova, I. G.; Jacobson, K. A. *Front. Drug Des. Discov.* **2007**, *3*, 63.
35. Molecular Operating Environment, in, C.C.G. Inc, 1255 University St., Suite 1600, Montreal, Quebec, Canada, H3B 3X3.
36. Kim, Y. C.; Ji, X. D.; Jacobson, K. A. *J. Med. Chem.* **1996**, *39*, 4142.
37. Stewart, J. J. *J. Comput. Aided Mol. Des.* **1990**, *4*, 1.
38. Dal Ben, D.; Lambertucci, C.; Taffi, S.; Vittori, S.; Volpini, R.; Cristalli, G.; Klotz, K.-N. *Purinergic Signalling.* **2006**, *2*, 589.
39. Volpini, R.; Dal Ben, D.; Lambertucci, C.; Taffi, S.; Vittori, S.; Klotz, K.-N.; Cristalli, G. *J. Med. Chem.* **2007**, *50*, 1222.
40. Volpini, R.; Buccioni, M.; Dal Ben, D.; Lambertucci, C.; Lammi, C.; Marucci, G.; Ramadori, A. T.; Klotz, K.-N.; Cristalli, G. *J. Med. Chem.* **2009**, *52*, 7897.
41. Dal Ben, D.; Buccioni, M.; Lambertucci, C.; Marucci, G.; Thomas, A.; Volpini, R.; Cristalli, G. *Bioorg. Med. Chem.* **2010**, *18*, 7923.
42. Mohamadi, F.; Richards, N. G. J.; Guida, W. C.; Liskamp, R.; Lipton, M.; Caufield, C.; Chang, G.; Hendrickson, T.; Still, W. C. *J. Comput. Chem.* **1990**, *11*, 440.
43. Cornell, W. D.; Cieplak, P.; Bayly, C. I.; Gould, I. R.; Merz, K. M.; Ferguson, D. M.; Spellmeyer, D. C.; Fox, T.; Caldwell, J. W.; Kollman, P. A. *J. Am. Chem. Soc.* **1995**, *117*, 5179.
44. Halgren, T. A. *J. Comput. Chem.* **1996**, *17*, 490.
45. Halgren, T. A. *J. Comput. Chem.* **1996**, *17*, 520.
46. Halgren, T. A. *J. Comput. Chem.* **1996**, *17*, 553.
47. Halgren, T. A. *J. Comput. Chem.* **1996**, *17*, 587.
48. Halgren, T. A. *J. Comput. Chem.* **1999**, *20*, 720.
49. Halgren, T. A. *J. Comput. Chem.* **1999**, *20*, 730.
50. Halgren, T. A.; Nachbar, R. *J. Comput. Chem.* **1996**, *17*, 616.
51. Dal Ben, D.; Buccioni, M.; Lambertucci, C.; Kachler, S.; Falgner, N.; Marucci, G.; Thomas, A.; Cristalli, G.; Volpini, R.; Klotz, K.-N. *Biochem. Pharmacol.* **2014**, *87*, 321.
52. Novellino, E.; Cosimelli, B.; Ehlardo, M.; Greco, G.; Iadanza, M.; Lavecchia, A.; Rimoli, M. G.; Sala, A.; Da Settimo, A.; Primofiore, G.; Da Settimo, F.; Taliani, S.; La Motta, C.; Klotz, K.-N.; Tuscano, D.; Trincavelli, M. L.; Martini, C. *J. Med. Chem.* **2005**, *48*, 8253.
53. Colotta, V.; Catarzi, D.; Varano, F.; Filacchioni, G.; Martini, C.; Trincavelli, L.; Lucacchini, A. *Bioorg. Med. Chem.* **2003**, *11*, 3541.
54. Nordstedt, C.; Fredholm, B. B. *Anal. Biochem.* **1990**, *189*, 231.
55. Cheng, Y. C.; Prusoff, W. H. *Biochem. Pharmacol.* **1973**, *22*, 3099.